

2007

Preliminary study on redundancy of a two-girder two-span continuous bridge under truck loads

Sarah E. Meagher
Lehigh University

Follow this and additional works at: <http://preserve.lehigh.edu/etd>

Recommended Citation

Meagher, Sarah E., "Preliminary study on redundancy of a two-girder two-span continuous bridge under truck loads" (2007). *Theses and Dissertations*. Paper 974.

This Thesis is brought to you for free and open access by Lehigh Preserve. It has been accepted for inclusion in Theses and Dissertations by an authorized administrator of Lehigh Preserve. For more information, please contact preserve@lehigh.edu.

Meagher, Sarah E.

**Preliminary Study
on Redundancy of a
Two-Girder Two-
Span Continuous
Bridge under Truck
Loads**

September 2007

Preliminary Study on Redundancy of a Two-Girder Two-Span
Continuous Bridge under Truck Loads

By

Sarah E. Meagher

A Thesis

Presented to the Graduate and Research Committee

of Lehigh University

in Candidacy for the Degree of

Master of Science

in

Structural Engineering

Lehigh University

September 2007

This thesis is accepted and approved in partial fulfillment of the requirements for the Master of Science.

5-21-07

Date

Dr. ~~Ben~~ T. Yen

Professor Emeritus

Thesis Advisor

Dr. Stephen P. Pessiki

Chairperson of Department

Acknowledgments

I would like to acknowledge the Advanced Technology for Large Structural Systems (ATLSS) Center and the Pennsylvania Infrastructure Technology Alliance (PITA) for funding this preliminary study and making my education at Lehigh University possible.

Thank you Dr. Ben T. Yen, the principal investigator for this research, for sharing your knowledge and providing support throughout my graduate education. Thank you for your constant encouragement and guidance in both my academic and professional endeavors. Thank you Dr. Richard Sause, the co-principal investigator for this research, for providing the opportunity and idea to work on this interesting project.

To Hussam Mahmoud, Ian Hodgson, and the members of the Infrastructure Monitoring Group, thank you for all your help with regards to finite element analysis techniques. I could not have completed this project without your guidance.

Lastly, I would like to thank my family and friends for providing the necessary support and encouragement throughout my entire experience at Lehigh University.

Table of Contents

| | |
|--|------|
| Acknowledgments | iii |
| Table of Contents | iv |
| List of Tables..... | vii |
| List of Figures | viii |
| Abstract | 1 |
| Chapter 1: Introduction | 2 |
| 1.1 Background | 2 |
| 1.2 Specifications and Related Research | 3 |
| 1.3 Research Objective..... | 7 |
| 1.4 Analysis Approach | 8 |
| 1.5 Overview of Report..... | 8 |
| Chapter 2: Development of Finite Element Model | 10 |
| 2.1 Introduction | 10 |
| 2.2 Model Geometry | 10 |
| 2.3 Assumptions..... | 14 |
| 2.4 Types of Elements Used..... | 16 |
| 2.5 Crack Stages..... | 21 |
| 2.5.1 Stage 2..... | 22 |
| 2.5.2 Stage 3..... | 23 |
| 2.6 Loading and Constraints | 24 |
| 2.6.1 Constraints | 25 |

| | |
|---|----|
| 2.6.2 Static Loading | 26 |
| 2.6.2.1 Dead Load | 26 |
| 2.6.2.2 Live Load | 27 |
| 2.6.3 Dynamic Loading..... | 28 |
| Chapter 3: Static Loading Analysis | 32 |
| 3.1 Introduction | 32 |
| 3.2 Stage 1 | 32 |
| 3.2.1 Stage 1 Dead Load Analysis | 32 |
| 3.2.2 Stage 1 Dead and Live Load Analysis | 35 |
| 3.3 Stage 2 | 38 |
| 3.3.1 Displacement..... | 38 |
| 3.3.2 Stress | 39 |
| 3.4 Stage 3 | 40 |
| 3.4.1 Displacement..... | 41 |
| 3.4.2 Stress | 42 |
| Chapter 4: Dynamic Loading Analysis | 44 |
| 4.1 Introduction | 44 |
| 4.2 Sudden Release of Crack | 44 |
| 4.2.1 Stage 2 Crack Release Dynamic Response..... | 45 |
| 4.2.2 Stage 3 Crack Release Dynamic Response..... | 49 |
| 4.3 Moving Truck Load | 54 |
| 4.3.1 Stage 1 Dynamic Response to the Moving Truck Load | 55 |
| 4.3.2 Stage 2 Dynamic Response to the Moving Truck Load | 56 |

| | |
|---|----|
| 4.3.3 Stage 3 Dynamic Response to the Moving Truck Load | 57 |
| Chapter 5: Bridge Response Comparison | 59 |
| 5.1 Introduction | 59 |
| 5.2 Amplification Factors..... | 59 |
| 5.3 Sudden Crack Release with Moving Truck Load | 62 |
| Chapter 6: Conclusions and Recommendations | 66 |
| 6.1 General Conclusions | 66 |
| 6.2 Stage 1 Conclusions | 66 |
| 6.3 Stage 2 Conclusions | 67 |
| 6.4 Stage 3 Conclusions | 68 |
| 6.5 Future Work | 69 |
| Appendix A: Two-Girder Two-Span Continuous Bridge Plans | 71 |
| References | 74 |
| Vita | 76 |

List of Tables

| | |
|---|----|
| Table 5.1: Maximum girder displacement values | 60 |
| Table 5.2: Amplification factors for the different analyzed loading conditions | 61 |
| Table 5.3: Amplification factor for the sudden crack release and moving truck load | 63 |

List of Figures

| | |
|--|----|
| Figure 2.1: Photograph of the Shippingport Bridge southern approach spans looking north | 11 |
| Figure 2.2: Photograph of bridge superstructure components | 13 |
| Figure 2.3: Various bridge components with the elemental representation in the computer model | 16 |
| Figure 2.4: Components modeled as shell elements as seen from the underside of the bridge | 17 |
| Figure 2.5: Bridge components represented by beam elements | 18 |
| Figure 2.6: Steel superstructure connection to concrete deck using rigid beam elements | 20 |
| Figure 2.7: Rigid beam elements connecting the deck, curb, and parapet | 21 |
| Figure 2.8: Stage 2 with flange crack | 23 |
| Figure 2.9: Stage 3 with flange and web cracked | 24 |
| Figure 2.10: Constraint conditions | 26 |
| Figure 2.11: Characteristics of AASHTO LRFD Bridge Specification HS-20 truck | 27 |
| Figure 2.12: Lane and load configuration | 28 |
| Figure 2.13: Time interval comparison for moving truck load | 31 |
| Figure 3.1: Stage 1 deflection due to dead load | 33 |
| Figure 3.2: Stage 1 contoured vertical deflection due to dead load | 33 |
| Figure 3.3: Stress contour in Stage 1 under dead load | 34 |

| | |
|---|----|
| Figure 3.4: Stage 1 girder deflection due to dead and live load..... | 35 |
| Figure 3.5: Stage 1 G1 dead load deflection versus dead and live load deflection..... | 36 |
| Figure 3.6: Stage 1 stringer and diaphragm deflection due to dead and live load..... | 36 |
| Figure 3.7: Stage 1 stresses at change in flange thickness due to dead and live load..... | 38 |
| Figure 3.8: G1 displacement comparison between Stage 1 and Stage 2 under dead and live load..... | 39 |
| Figure 3.9: Stress near the crack at Stage 2 | 40 |
| Figure 3.10: Deflection contours under Stage 3 cracking with dead and live load..... | 41 |
| Figure 3.11: G1 displacement comparison between Stage 1, 2, and 3 under dead and live load..... | 42 |
| Figure 3.12: Concrete region failing for Stage 3 cracking under static dead and live load | 43 |
| Figure 4.1: Displacement response to the dynamic release of crack at all Stage 2 time increments | 46 |
| Figure 4.2: Maximum dynamic displacement response to Stage 2 crack release varying with time | 47 |
| Figure 4.3: Stage 2 sudden crack release displacement versus Stage 2 static crack displacement | 48 |

| | |
|--|----|
| Figure 4.4: Displacement response to the dynamic release of crack at all Stage 3 time increments | 50 |
| Figure 4.5: Maximum dynamic displacement response to the release of Stage 3 at selected time increments..... | 51 |
| Figure 4.6: Maximum dynamic displacement response to Stage 3 crack release varying with time | 52 |
| Figure 4.7: Stage 3 sudden crack release displacement versus Stage 3 static crack displacement | 53 |
| Figure 4.8: Stage 1 dynamic response of displacement at 56'-3" from the south abutment due to the moving truck load | 55 |
| Figure 4.9: Stage 2 dynamic response of displacement at 56'-3" from the south abutment due to the moving truck load | 56 |
| Figure 4.10: Stage 3 dynamic displacement response at the southern crack location to the moving truck load..... | 58 |
| Figure 5.1: Estimated yielding region for Stage 3 combined crack release and moving truck load..... | 64 |

Abstract

Bridges termed “fracture-critical” are defined in the AASHTO LRFD Bridge Design Specifications as consisting of a fracture-critical member (FCM) whose failure is expected to result in the collapse of the bridge (AASHTO, 2005). In order to avoid such a complete bridge failure, AASHTO recognizes the need for redundancy. However, the basis for defining the redundancy of two-girder bridges has been uncertain for bridge engineers for many years.

This preliminary study investigates how susceptible a two-girder bridge is to collapse from the loss of a girder (FCM). An in-depth three dimensional finite element model of a two-girder two-span continuous bridge is created. The finite element model analyses involve static loading, static conditions with open crack, dynamic moving load, dynamic fracture, and a combination of both dynamic moving load and dynamic fracture. All analyses are conducted for three stages of crack length: no crack, flange crack in girder, and full depth crack to the top of the girder web.

The two-girder two-span continuous bridge is examined for regions of yielding in the steel superstructure and loss of concrete deck due to failure. It is found that the displacement and stresses of the bridge with a crack and under a moving truck load could be approximated by those under the corresponding static load. For any of the cases analyzed, the bridge remains capable of carrying an HS-20 truck and is behaving redundantly with a crack in a girder.

Chapter 1: Introduction

1.1 Background

This preliminary study investigates a two-girder two-span continuous deck bridge typical of two-girder bridges in Pennsylvania that is considered critical with respect to redundancy and potential collapse. This type of bridge is termed “fracture-critical” and is defined in the AASHTO LRFD Bridge Design Specifications as “consisting of a fracture-critical member (FCM) or component in tension whose failure is expected to result in the collapse of the bridge or the inability of the bridge to perform its function” (AASHTO, 2005). In order to avoid such a complete bridge failure, AASHTO recognizes the need for redundancy, or in other words, “the quality of a bridge that enables it to perform its design function in a damaged state” (AASHTO, 2005). This includes the redistribution of load previously carried by the failed member. The specification classifies two-girder bridges as non-redundant and fracture-critical. However, it has been shown in previous research (Daniels, 1989) that despite this classification, two-girder bridges have demonstrated redundancy.

There are numerous examples of bridges considered fracture-critical that have fractured, but not collapsed. The Lafayette Street Bridge in St. Paul, Minnesota experienced a full-depth fracture of a girder in 1976. The bridge did sag 6.5 in., but did not collapse. In 1977, a full-depth fracture occurred in the I-79 Bridge at Neville Island in Pittsburgh, Pennsylvania. There was almost no observable deflection and the bridge continued in-service for some time before the fracture was noticed. This

was also true for the 2003 fracture of the US-422 Bridge near Pottstown, Pennsylvania. The entire bottom flange and about 9 in. of the web fractured, but there was no appreciable deflection. These examples illustrate that despite the fracture-critical designation for these two-girder bridges, other elements, such as the deck, floorbeams, bracing, and stringers, provide alternate load paths that can carry the bridge loads to prevent collapse. (Connor, 2005)

The basis for defining the redundancy of two-girder bridges has been uncertain for bridge engineers for many years. The AASHTO specifications do not provide any specific guidelines for design or evaluation of redundancy in bridges. Since it is absolutely necessary to avoid collapse of two-girder bridges due to fracture of one girder, the fracture-critical specification has resulted in a tendency to be on the conservative side in evaluation of new and existing two-girder bridges. The result of this is more costly new bridges and more expensive inspection and maintenance of existing bridges. It has been estimated that the approximate initial cost premium for new bridges with FCMs is about 8% of the cost of fabricated steel. The cost of the fracture-critical inspection is typically on the order of two to five times greater than inspections for bridges without FCMs (Connor, 2005). It is clear that specific provisions for after-fracture redundancy are a necessary addition to the AASHTO LRFD Bridge Design Specifications.

1.2 Specifications and Related Research

Fracture-critical members are nonredundant. However, as shown by the examples of fracture-critical bridges not collapsing after fracture, the present practice of categorizing the non-redundancy of a two-girder bridge appears to be inaccurate.

AASHTO LRFD Bridge Design Specifications define redundancy as “the quality of a bridge that enables it to perform its design function in a damaged state.”

It offers the following information on bridge redundancy in Article 1.3.4:

Multiple-load-path and continuous structures should be used unless there are compelling reasons not to use them.

Main elements and components whose failure is expected to cause the collapse of the bridge shall be designated as failure-critical and the associated structural system as nonredundant. Alternatively, failure-critical members in tension may be designated fracture-critical.

Those elements and components whose failure is not expected to cause collapse of the bridge shall be designated as nonfailure-critical and the associated structure system as redundant.

Section 6.6.2 of the AASHTO LRFD Bridge Design Specifications permits the completion of an in-depth analysis of a bridge to account for the strength of fracture-critical members in their damaged condition. The commentary of this section states that:

The criteria for refined analysis used to demonstrate that part of the structure is not fracture-critical has not yet been codified. Therefore, the loading cases to be studied, location of potential cracks, degree to which the dynamic effects associated with a fracture are included in the analysis, and fineness of models and choice of element type should all be agreed upon by the Owner and the Engineer. The ability of a particular software product to adequately capture the complexity of the problem should also be considered and the choice of software should be mutually agreed upon by the Owner and the Engineer. Relief from the full factored loads associated with the Strength I Load Combination of Table 3.4.1-1 should be considered, as should the number of loaded design lanes versus the number of striped traffic lanes.

Much research has been done in the area of redundancy to help increase the knowledge pool for the specifications. This research includes finite-element analysis simulations that test the after-fracture behavior of fracture-critical bridges. Ghosn

and Moses (1994) define four critical limit states that ensure a girder bridge is redundant with respect to both individual member behavior and structural system behavior, while current guidelines ignore the difference and combination between the two. The four critical states (defined by load multipliers) are determined for any bridge configuration using three-dimensional finite element analysis with loading consisting of two AASHTO HS-20 vehicles. LF_1 is defined as the number of HS-20 trucks required for first member failure and is determined from a linear elastic structural model of the bridge while incrementing the loads. The ultimate capacity limit, LF_u , is defined as the maximum possible truck load applied until bridge failure. This is done using a nonlinear structural model of the bridge and incrementing the load. The system serviceability limit state, LF_s , is expressed in terms of the number of HS-20 trucks that can be placed on the structure, using a nonlinear analysis, before the displacement limit of span length/200 is reached. The load multiplier corresponding to the ultimate capacity of the damaged structure is defined as LF_d . This multiplier is determined by analyzing a nonlinear structural model of the damaged bridge (fracture-critical member removed) and incrementing the truck loads until the system collapses. A comparison is made between the load multipliers to measure the level of bridge redundancy. The system reserve ratios for the ultimate limit state $R_u (LF_u/LF_1)$, for the serviceability limit state $R_s (LF_s/LF_1)$, and for the damaged condition $R_d (LF_d/LF_1)$ are nominal (deterministic) measures of bridge redundancy. To calibrate the load multipliers, a number of different bridges and configurations were studied. Tables were then generated for the type of bridge and

2

its respective configuration (includes number of beams and beam spacing). These tables provide the limits for redundancy for the different load multipliers.

Heins and Kato (1982) considered three basic two-girder space frame models to study the effect of lateral bracing. The models include an uncracked girder, cracked girder without bottom lateral bracing, and cracked girder with bottom lateral bracing. Dead load was not considered and live load consisted of two HS-20 trucks. The results from this study found that the deflection of the cracked girder was substantially reduced when bracing was used due to the effect of bracing on load distribution. Heins and Hou (1980) studied the effect of bracing members on load distribution of two-girder and multigirder systems. They accomplished this by analyzing a space frame model of the bridges after the development of a crack in one of the girders. The analyses resulted in the following conclusions: bracing and diaphragms reduced the deflection from 5-10% for uncracked systems, the deflection after one crack develops increases by 40% (two-girder system) and 10% (multigirder system) when no bracing is used, and the deflection increases by 10% if bracing is considered for the cracked condition.

Lai (1994) studies the redundancy of a tied-arch bridge using a three dimensional finite element computer model. Tied-arch bridges are designated fracture-critical because it is assumed that if one of the two ties fractures, the bridge will collapse. Analyzing the bridge using static load increments resulted in it being able to carry the full dead load plus a live load of 130% HS-20 loading when one tie is totally fractured. The deck slab will however need to be retrofitted because it was no longer serviceable. The linear elastic dynamic analysis that considers an impulse

effect due to sudden fracture of a tie results in a much higher magnification factor. Lai suggests that “an after-fracture redundancy study look into the dynamic and impulse effect due to brittle fracture of any structural component, if brittle fracture is a potential danger.”

1.3 Research Objective

The objective of this research is to investigate if a bridge traditionally classified as fracture critical can actually be shown to be redundant. This involves studying a two-girder, two-span continuous bridge using finite element analysis under different stages of crack size for both static and dynamic loading as well as static and dynamic fracture. It is especially important that dynamic loading analysis is considered because much previous research has mostly concentrated on static loading analysis. Goals of this research include investigation of stress distribution, identifying critical secondary members to the after-fracture redundancy of the bridge, and the possibility of drastic deflection.

Approximately 11% of the steel bridges in the United States have FCMs. Most of these (83%) are two-girder bridges and two-line trusses (Connor, 2005). Although the specific bridge studied under finite element analysis is but one example of these bridges, it is typical of the other 9% of two-girder bridges in the US. It is anticipated that this bridge, although designated as fracture critical, will behave redundantly.

1.4 Analysis Approach

The approach to obtaining these research objectives begins with selecting a bridge typical of two-girder bridges in the US. The chosen bridge is a part of the Shippingport Bridge, which is located in Beaver County, Pennsylvania and spans the Ohio River. The main river crossing consists of a three-span combined deck/through truss. The southern approach to the bridge meets the typical specifications of a two-girder two-span unit. A complete three dimensional finite element model is created using this bridge as a template while modifying certain aspects, such as making the steel superstructure composite with the deck.

Three stages of simulated crack located at a change in girder flange thickness are incorporated in the finite element model. These stages are a model with no crack, a cracked bottom flange plate, and a full depth crack to the top of the web. Two loading conditions are applied at each of these stages: simulated static and dynamic loads from an HS-20 truck. The sudden release of internal forces (dynamic crack fracture) is also investigated.

It is anticipated that the analytical results of stresses and displacements can be compared with the material strength and serviceability load carrying limits. The possibility of buckling or yielding of affected secondary members will also be evaluated.

1.5 Overview of Report

Chapter 2 describes the development of the finite element model. An overall description of the bridge that the model is based on is also presented. All

components of the finite element model are explained in detail. These include assumptions, types of elements used, the three assumed stages of fracture, constraints, and all loading conditions considered.

The static loading analyses for the three stages of fracture are discussed in Chapter 3. Chapter 4 contains the dynamic loading analyses. These loading analyses consist of the simulated sudden dynamic fracture and the dynamic moving HS-20 truck load.

Chapter 5 compares the different analysis cases and provides a basis for approximating other loading analyses. A summary of the conclusions from the preliminary study is in Chapter 6, as well as recommendations for future work.

Chapter 2: Development of Finite Element Model

2.1 Introduction

The program FEMAP (Finite Element Modeling And Postprocessing) version 8.3 is used to generate a three-dimensional model of the Shippingport Bridge southern approach spans. FEMAP is used for the pre- and post-processing applications of the study. Once built, the models are analyzed using ABAQUS 6.6-1, a general purpose finite element analysis program. The purpose of Chapter 2 is to discuss the finite element modeling process of the two-girder two-span continuous approach to the Shippingport Bridge in Beaver County, Pennsylvania.

2.2 Model Geometry

As stated in Chapter 1, the purpose of the preliminary study is to investigate a two-girder two-span continuous deck bridge typical of two-girder bridges in Pennsylvania. A “typical” two-girder bridge is one that includes spans greater than 100 ft., floorbeams framing into the girders, stringers supporting the deck, secondary members (diaphragms and lateral bracing), composite action with the deck, simple-supported constraints, and symmetry between the spans as well as across the centerline. One bridge that fits most of the “typical” two-girder bridge mold is the southern approach spans to the Shippingport Bridge. It was built in 1961 and spans the Ohio River connecting the boroughs of Shippingport to the south and Midland to the north. A photograph of the bridge including a portion of the main river combined deck/through truss is shown in Figure 2.1.

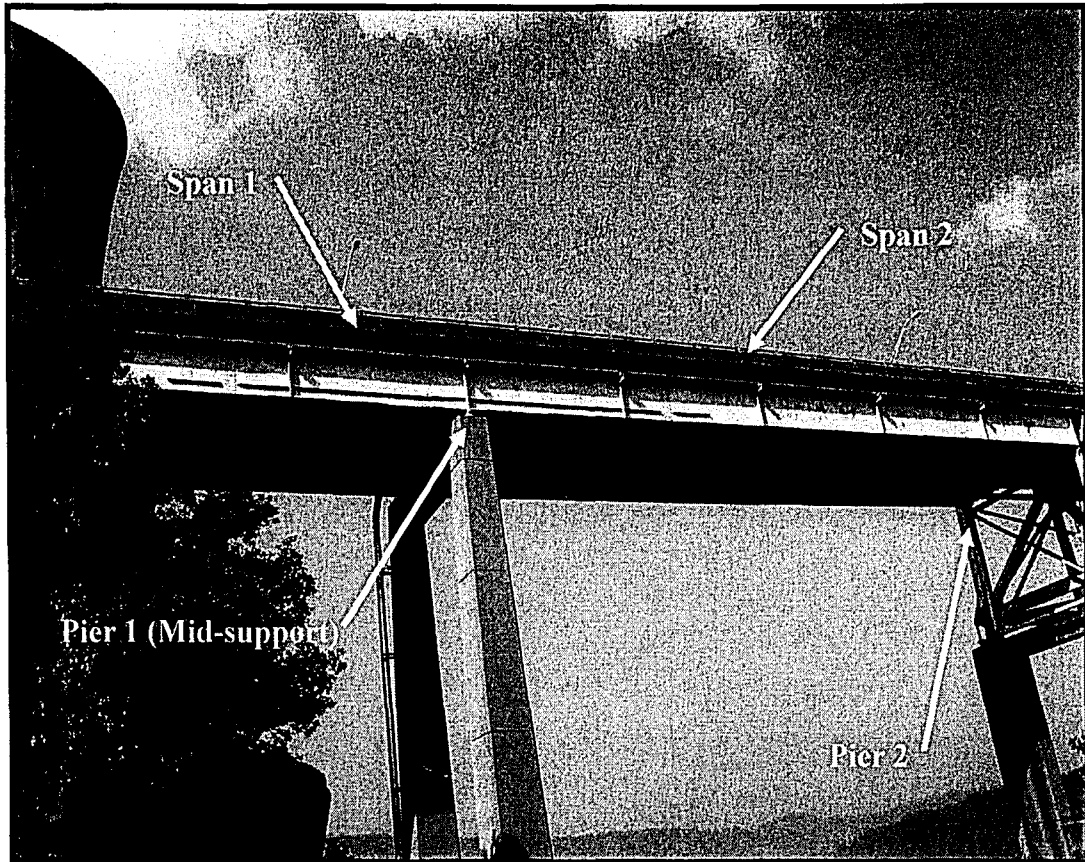


Figure 2.1: Photograph of the Shippingport Bridge southern approach spans looking north

The Shippingport southern approach spans include most of the components necessary for a “typical” two-girder bridge in Pennsylvania. However, some modifications are made to the geometry, material specifications, and component interaction. The purpose of the preliminary study is not to focus on the Shippingport approach spans, but instead to use the geometry as a foundation for a more modern “typical” two-girder two-span continuous bridge.

The two major modifications made to the approach spans are done in order to update the bridge to more modern specifications. The first modification changes the deck to be composite with the superstructure. The second modification changes the originally specified steel (A373 Grade 32) and concrete (Class AA) to more modern

materials. These are A572 Grade 50 steel and standard concrete with a compressive strength of 3.5 ksi.

The two-girder two-span continuous bridge consists of two 125' spans beginning at the southern approach. These spans are designated as Span 1 and Span 2, respectively. Span 1 is symmetrical to Span 2 across the mid-support designated as Pier 1. Therefore, only the geometry of the first span is discussed, as the second span is the same. The plate girders are 99" deep and have varying flange thickness along the length of the bridge from 7/8" to 2-5/8". Longitudinal stiffeners are located in the compression regions along the girders. Intermediate stiffeners, on the opposite side of the girder web from the longitudinal stiffeners, are located along the entire length of the girders at varying spacing. All intermediate stiffeners are cut short of the tension flange of the girder except the stiffeners at the floorbeam to girder connections. Field splices are located at the theoretical dead load inflection points. These splices are not included in the two-girder two-span continuous bridge in order to increase the efficiency of modeling.

Floorbeams are located at each support and every 25' in between. The floorbeams have a 54" web depth and have the same configuration at all locations except at the two end supports. They have a flange thickness of 1/2" instead of 1" at all other locations. The connection between the floorbeam and girder is formed by welding the floorbeams's bottom flange to a lateral gusset plate and bolting the floorbeam web to the girder stiffener. It is assumed that all welds and bolts throughout the model produce complete attachment. The four longitudinal stringers (21WF55) are spaced at 6' and are bolted to the top flange of the floorbeam flanges.

Diaphragms, either 12C20.7 or 18WF50 depending on location, are located transversely, halfway between the floorbeams. These are bolted to the stringers using a connection plate. The diaphragms provide support to the lateral bracing members at midpoint. The lateral bracing, L6"x6"x7/16", is attached to the same lateral gusset plates that the floorbeam bottom flanges are welded too. A photograph of the underside of the bridge with all the accompanying components is shown in Figure 2.2.

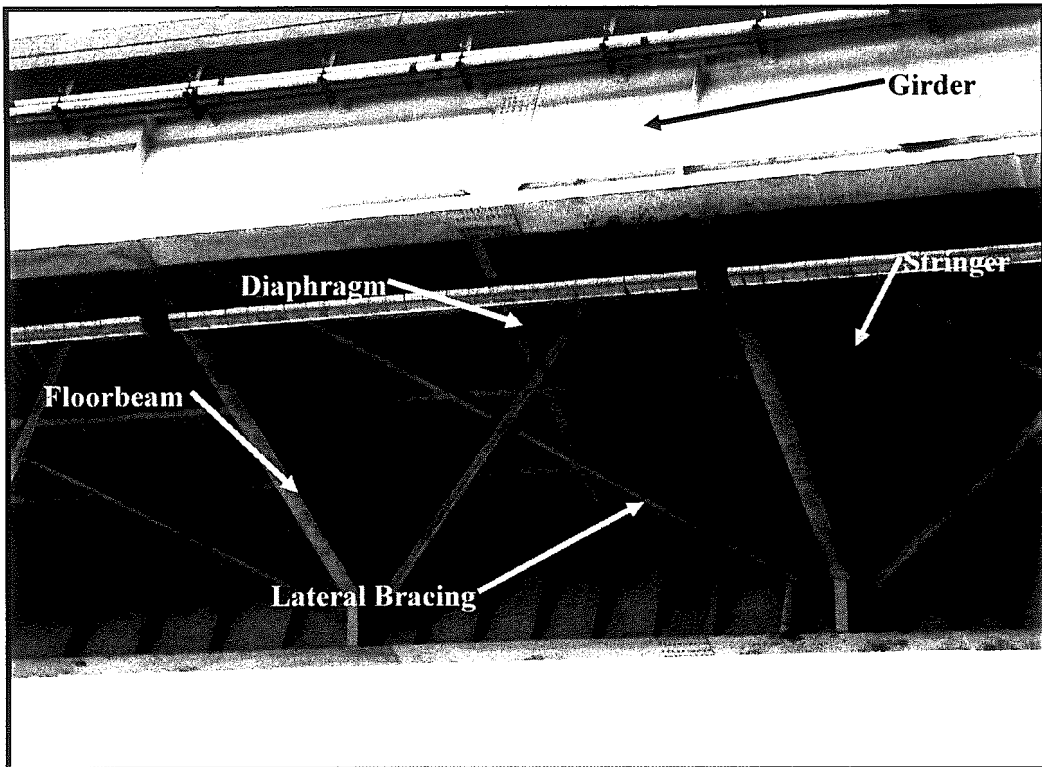


Figure 2.2: Photograph of bridge superstructure components

The concrete deck is typically 7" thick and extends transversely 3'-3" beyond the web of the girder. The curb and parapet dimensions are slightly changed in order to more easily create the model. However, the volume is the same as originally

specified. All the concrete is assumed to have a standard weight of 150 lb/ft^3 while all steel is assumed to have a standard weight of 490 lb/ft^3 . Complete plans for the model can be found in Appendix A.

2.3 Assumptions

There are many assumptions made for the computer model representation of the two-girder two-span continuous bridge. The three main areas of assumptions are in regards to geometry, material specifications, and component connection.

The two major assumptions made with respect to model geometry are assuming the deck acts compositely with the superstructure and assuming the bridge is symmetrical about Pier 1 (mid-support) as well as the centerline of the bridge. Making the deck composite with the superstructure is necessary in order to update the bridge interaction to modern design. The purpose of the preliminary study is to provide more information about after-fracture redundancy to current practicing engineers and code writing organizations. Practically all bridges constructed after the 1970's are designed to be composite with the deck and it is therefore unrealistic to assume otherwise. Also, it is expected that the composite deck will enhance the after-fracture redundancy of the bridge structure. The concrete deck is conservatively assumed to have no steel reinforcement. Although not in accordance with current bridge designs, the exclusion of steel reinforcement reduces the complexity of the bridge model.

Making the two-girder two-span continuous bridge symmetrical about the mid-support as well as along the centerline of the bridge eases the complication of modeling the bridge. Although this condition of double symmetry does not exist in

all two-girder bridges, it is the case in many. The differences between the spans and across the centerline in the Shippingport plans are so minimal that making the bridge symmetrical is expected to have only minimal effect on the after-fracture behavior of that bridge.

As stated in the above model geometry section, other specific geometrical assumptions are made. All welded and bolted connections are assumed to create complete attachment. The field splices located at the inflection points on the girders are ignored and the girders are assumed to have continuous web and flange plates. The lateral bracing members are connected to the end corner of the lateral gusset plates instead of bolted at numerous points of the plate. This may create local buckling of the gusset plate, but is ignored as the global behavior of the bridge is primarily being studied. The parapet and curb geometry is changed slightly in order to more easily create the model. However, the volume of concrete for these components is kept the same.

The materials are changed from the originally specified steel (A373 Grade 32) and concrete (Class AA) to more modern materials. This is done for the same reasons as making the deck composite with the superstructure. These adopted materials are A572 Grade 50 steel and standard concrete with a compressive strength of 3.5 ksi.

The last major assumption concerns the connection of different superstructure components. For example, the floorbeam web (3/8" thick) is bolted to a stiffener (5/8" thick) on the girder. However, in the computer model, the overlapping components are combined as one plate with a thickness of 1".

2.4 Types of Elements Used

There are three different types of elements used to create the finite element model of the two-girder two-span continuous bridge. These elements are shell elements, beam elements, and rigid elements. ABAQUS 2006 has an extensive element library and each type of element has specific capabilities. The above three elements are chosen to represent the behavior of specific components of the real structure and for the type of analysis completed. An illustration of one section of the bridge model without the deck looking northwest can be seen in Figure 2.3.

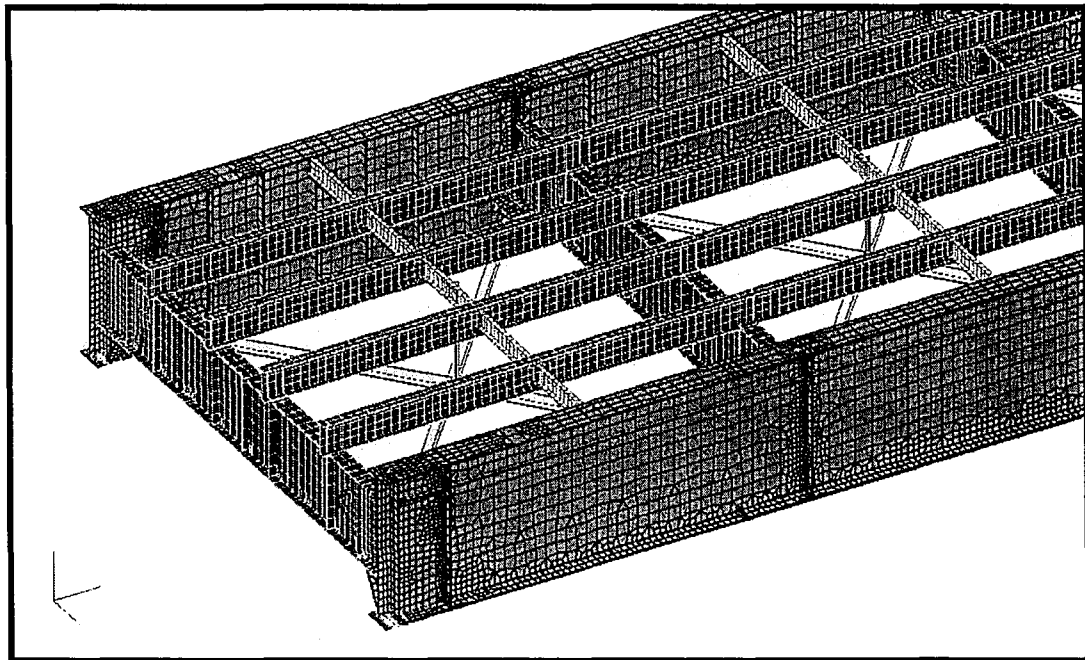


Figure 2.3: Various bridge components with the elemental representation in the computer model

Most of the finite element model is comprised of 8-noded parabolic “thick” shell elements (S8R). Shell elements have curved inner and outer surfaces with a thickness that is small in comparison with the overall dimensions of the shell. The 8-noded quadratic element is a stress/displacement element with reduced integration

and uses six degrees of freedom per node (three displacement components and three rotation components). The S8R shell element is used to represent all plate components of the model except for the lateral bracing and in some instances where a rigid connection between shell elements is necessary. The structural components represented by shell elements include the girders, floorbeams, diaphragms, stringers, concrete deck, parapet, and curb. Figure 2.4 illustrates the components modeled as shell elements.

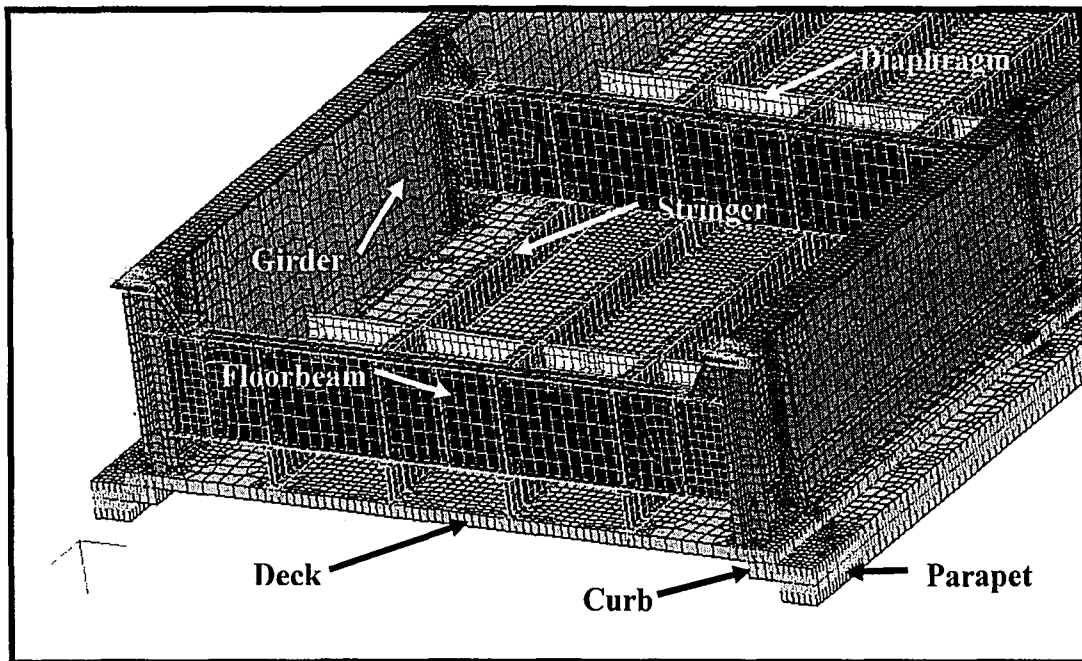


Figure 2.4: Components modeled as shell elements as seen from the underside of the bridge

The shell elements representing steel plates are assigned isotropic material properties equivalent to A572 Grade 50 steel, with specified yield strength of 50 ksi, elastic modulus of 29,000 ksi, and weight density of 490 lb/ft³. The shell elements representing the concrete components are assigned an isotropic material property with a compressive strength of 3.5 ksi and an elastic modulus of 3,372 ksi. The assumed weight density for concrete is the standard 150 lb/ft³.

Beam elements are used in the computer model to represent the lateral bracing members as well as the vertical connection between the lateral bracing members and the diaphragms. Figure 2.5 illustrates the bridge components represented by beam elements.

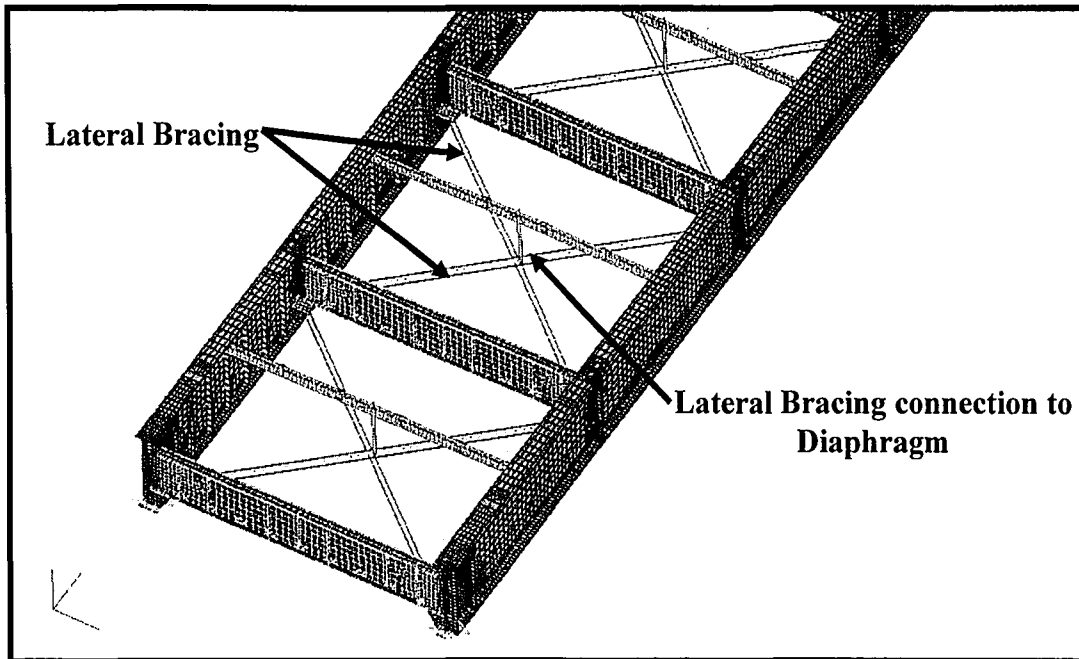


Figure 2.5: Bridge components represented by beam elements

The type of beam element chosen to represent these bridge components is different for each. The elements representing the lateral bracing are 2-noded linear beam elements and the elements representing the connection between the lateral bracing members and the diaphragms are 3-noded quadratic beam elements. Both types of the beam elements are termed “Timoshenko” (shear flexible) elements which allow for transverse shear deformation and also have six degrees of freedom at each node (three translations and three rotations). Allowing transverse shear deformation means that the cross-section may not necessarily remain normal to the beam axis. This is important for possible out-of-plane bending and local buckling of

the lateral bracing members and the vertical connection between the lateral bracing members and diaphragms as the crack in the girder progresses. As with the shell elements representing the steel plates, the beam elements are assigned isotropic material properties equivalent to A572 Grade 50 steel. The specified yield strength is 50 ksi, elastic modulus is 29,000 ksi, and weight density is 490 lb/ft³.

Rigid beam or multi-point constraints (MPC) elements are used to model two different connections in the finite element model of the two-girder two-span continuous bridge. The first connection is between the steel plate shell elements and the concrete deck shell elements. This connection is used to represent the composite action of the steel superstructure with the concrete deck. This connection occurs between the girders and stringers and the concrete deck directly above and along the length of the bridge. This connection is presented in Figure 2.6 without the shell thickness shown so the MPC's can be more visible.

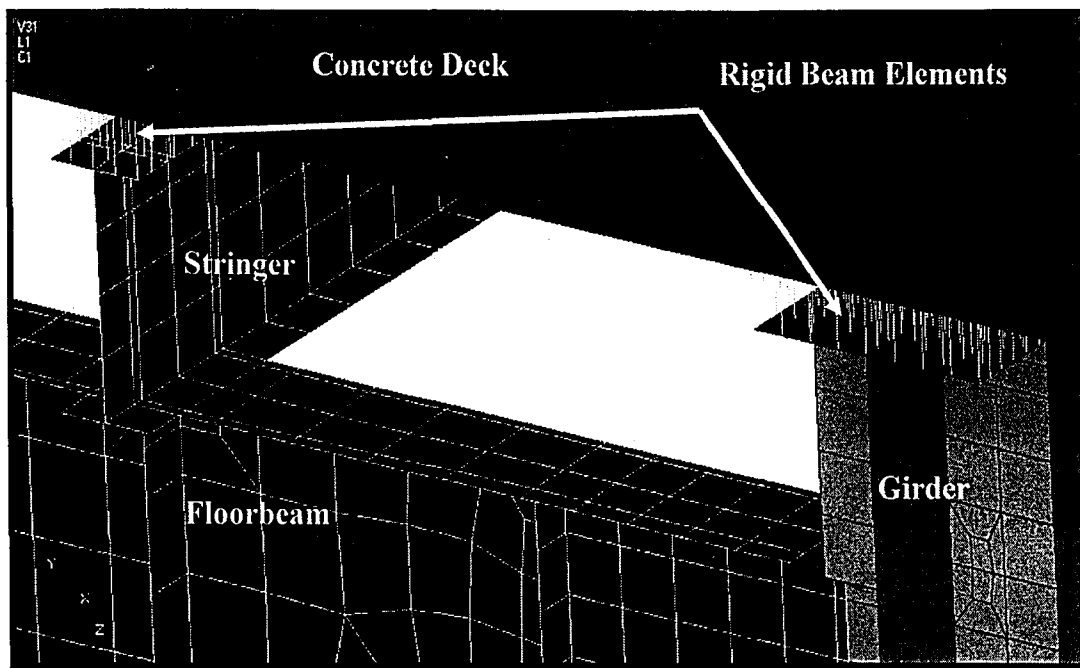


Figure 2.6: Steel superstructure connection to concrete deck using rigid beam elements

The second connection is between the parapet, curb, and deck shell elements. Rigid beam elements are used for this connection since the parapet shell elements are positioned directly above the curb shell elements which are in turn positioned directly above the deck shell elements. Figure 2.7 illustrates this connection between the concrete elements with the shell element thicknesses shown.

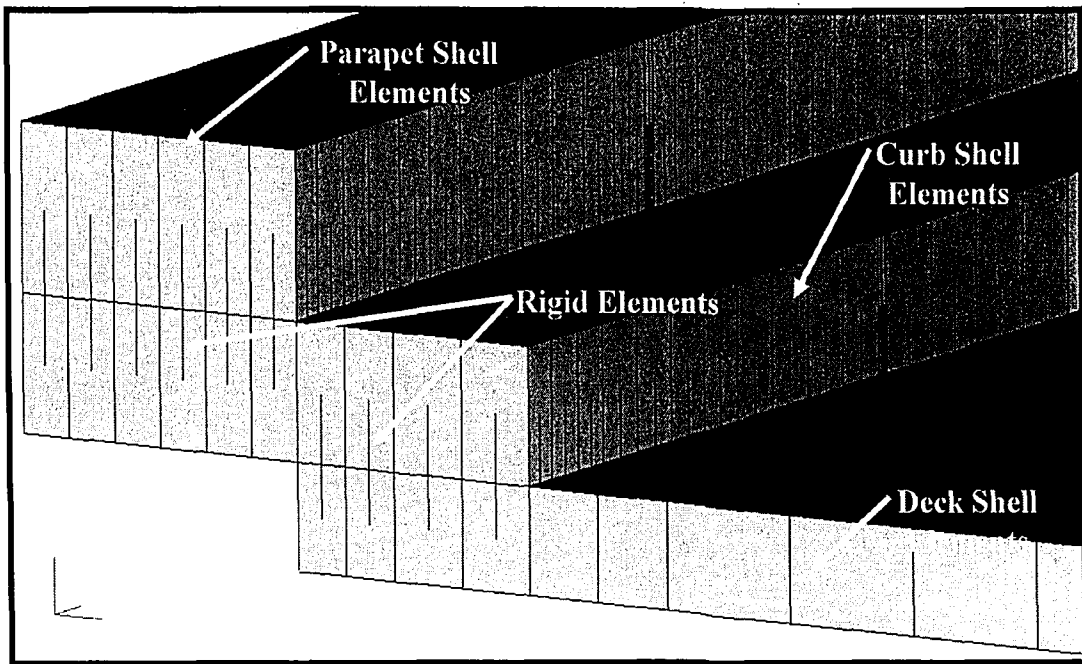


Figure 2.7: Rigid beam elements connecting the deck, curb, and parapet

Rigid elements connect two nodes whose total motion (of all six degrees of freedom) is governed by the motion of a single node, called the independent or reference node. In Figure 2.6 the reference nodes are located on the bridge steel components and the slave nodes (dependent nodes) are located on the deck. In Figure 2.7 reference nodes for the deck to curb connection are located on the deck and for the curb to parapet connection are located on the curb. The rigid element transfers all axial, shear, and bending forces from the reference (master) node to the connected slave node, but has no mass itself. These assumptions are necessary for modeling the composite action of the two-girder two-span continuous bridge.

2.5 Crack Stages

There are three stages of simulated crack at a judicially chosen cross section of one girder. The chosen location is 77 ft from the south abutment where there is a

change in girder flange thickness from 1-1/2" to 7/8". This cross section is not necessarily the only location where a fracture could occur, nor is it the location that a fracture will definitely occur. It is a location that a fracture might occur and the after-fracture redundancy behavior of the bridge is representative of other fracture locations. A cross section of a floorbeam could also be a likely location. In-service fractures of bridges provide examples of other fracture locations. The Lafayette Street Bridge, a two-girder three-span continuous bridge, experienced a full-depth fracture of a girder at a floorbeam connection at 118'-8" of the 362' middle span (Fisher, 1984).

There are a couple of reasons that make the chosen cross section for the simulated crack a likely location for fracture. The first reason is that the crack cross section is located about 2/3rd along the span length where the change of live load moment is large. The second reason is that the change in flange thickness could introduce flaws due to the weld at that location. The initial flaw and stress concentration at the change of flange thickness could start fatigue cracking, leading to fracture under adverse conditions.

The first simulated stage of cracking Stage 1, assumes that the bridge cross section is intact and that there is in fact no cracking. Stage 1 is the base case for all analysis and comparison.

2.5.1 Stage 2

Stage 2 cracking simulates a completely cracked flange plate. This stage is an intermediate step and is analyzed for comparison with Stages 1 and 3. Cases of flange cracks indicate that the tension flange is usually not completely severed at the

onset of Stage 3. Assuming a completely cracked tension flange plate exaggerates the damage for the examination of fracture redundancy at this intermediate stage.

Stage 2 cracking is created by not merging the flange nodes from the elements on either side of the crack location at 77 ft from the south abutment. This creates an unconnected region that imitates an immediate fracture of the bottom flange of the girder. It is to be noted that the purpose of the preliminary study is not to examine how this crack is propagating, but to explore the redundancy of the bridge structure after the fracture of a member. Complete fracture of the flange permits a relatively easier modeling process. The region of the model with the flange crack is shown in Figure 2.8.

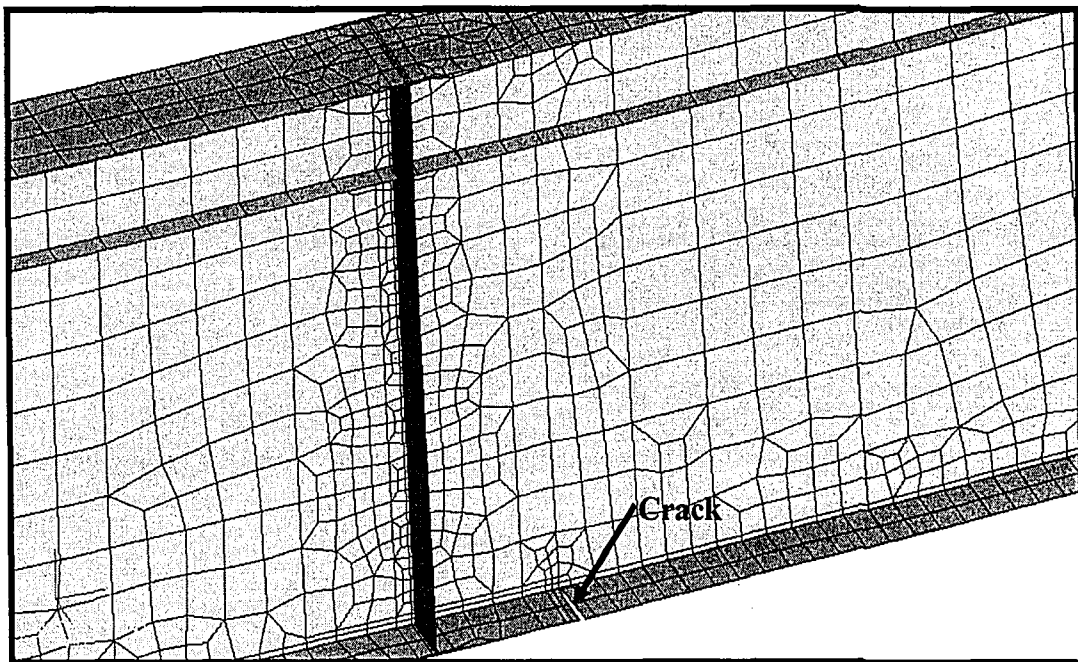


Figure 2.8: Stage 2 with flange crack

2.5.2 Stage 3

Stage 3 cracking simulates a full depth crack to the bottom of the top flange and is a worse case scenario. Common belief is that this worse case scenario will

lead to complete failure or collapse of the bridge due to the non-redundant nature of a two-girder bridge. However, it is the premise of this preliminary study that two-girder bridges are much more redundant than assumed by AASHTO. To evaluate the displacement and stress of the two-girder two-span continuous bridge under a full depth crack should provide information for judgment.

Stage 3 cracking is created by not merging the flange, web, and longitudinal stiffener nodes from the elements on either side of the crack location. This creates an unconnected region that imitates an immediate fracture from the bottom of the girder to the top of the web. Figure 2.9 shows the after fracture view of the stage 3 crack in the girder.

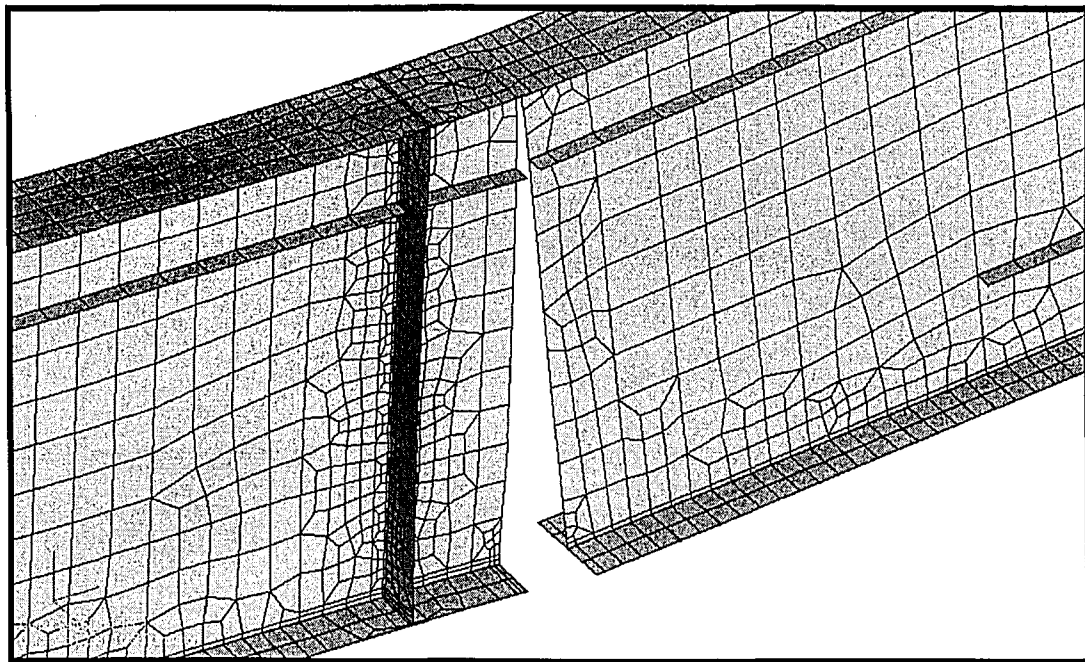


Figure 2.9: Stage 3 with flange and web cracked

2.6 Loading and Constraints

The model of the two-girder two-span continuous bridge utilizes simplified constraints and loading conditions. The constraints are idealized as simply supported

(pin-roller) in all directions. The loading includes dead load, which consists of the weight of the various structural members on the bridge, and live load, which is represented by an HS-20 design truck.

2.6.1 Constraints

The constraints are idealized as simply supported in order to allow freedom for rotation and displacement at the supports. The stiffness towards rotation and displacement, owing to friction and material behavior of the bearings, is ignored to allow for a worse case scenario.

The model of the two-girder two-span continuous bridge is a three dimensional model symmetrical across the mid-supports as well as in the transverse direction. In order to accommodate the symmetry in two directions, the movement in the transverse direction is treated separately from that in the longitudinal direction. In the transverse direction, G1 is assigned all pin connections and G2 is assigned all roller connections. See Appendix A for bridge configuration labeling. This allows the floorbeams in the transverse direction to act simply supported. In the longitudinal direction, both girders are assigned a roller connection at the south abutment, a pin connection at the mid-support (Pier 1), and a roller connection at Pier 2. This allows both spans in the longitudinal direction to act simply supported. Figure 2.10 presents a diagram of the directional support conditions and how they allow certain directional movement.

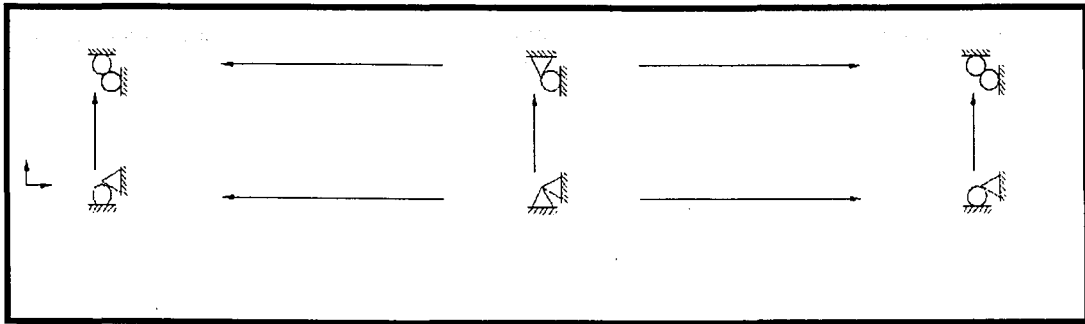


Figure 2.10: Constraint conditions

2.6.2 Static Loading

Static loading on the two-girder two-span continuous bridge consists of the weight of all the structural members or dead load (DL) and an HS-20 truck or live load (LL).

2.6.2.1 Dead Load

The weight of the dead load for the two-girder two-span continuous bridge is 1,347,204 lb. This comes from assigning a density of 490 lb/ft³ to all the steel components and a density of 150 lb/ft³ to all the concrete components. These values can be converted to mass densities by changing the lb/ft³ units to lb/in³ and dividing by gravity, g (386.4 in/s²). After applying these changes the mass density for steel and concrete, respectively, are 7.3386×10^{-4} lb-s²/in⁴ and 2.2465×10^{-4} lb-s²/in⁴. The mass density values are then specified in the FEMAP model for their respective material properties. Based on this, each element is allocated a portion of the dead load based on its volume of material. As a result, the dead load throughout the two-girder two-span continuous bridge model is an elemental distributed load.

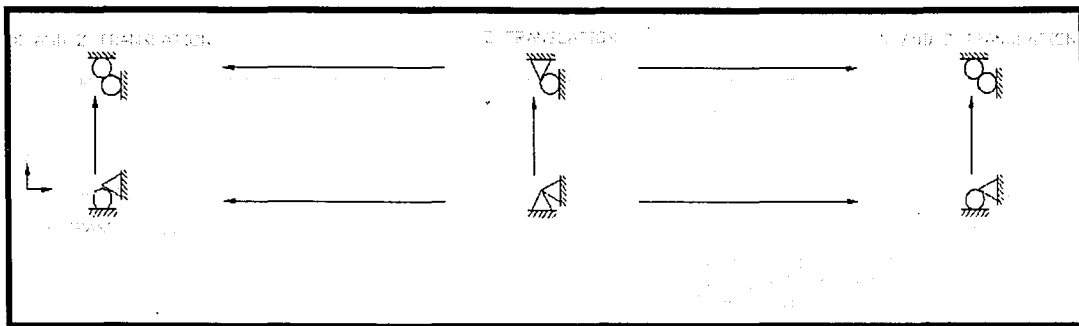


Figure 2.10: Constraint conditions

2.6.2 Static Loading

Static loading on the two-girder two-span continuous bridge consists of the weight of all the structural members or dead load (DL) and an HS-20 truck or live load (LL).

2.6.2.1 Dead Load

The weight of the dead load for the two-girder two-span continuous bridge is 1,347,204 lb. This comes from assigning a density of 490 lb/ft³ to all the steel components and a density of 150 lb/ft³ to all the concrete components. These values can be converted to mass densities by changing the lb/ft³ units to lb/in³ and dividing by gravity, g (386.4 in/s²). After applying these changes the mass density for steel and concrete, respectively, are 7.3386×10^{-4} lb-s²/in⁴ and 2.2465×10^{-4} lb-s²/in⁴. The mass density values are then specified in the FEMAP model for their respective material properties. Based on this, each element is allocated a portion of the dead load based on its volume of material. As a result, the dead load throughout the two-girder two-span continuous bridge model is an elemental distributed load.

2.6.2.2 Live Load

Live load on the two-girder two-span continuous bridge consists of an HS-20 truck. The HS-20 truck is the specified design truck in the AASHTO LRFD Bridge Design Specifications. The weights and spacings of axles and wheels for the design truck are illustrated in Figure 2.11. As shown in Figure 2.11, the front wheel axle weighs 8 kip and the two rear axles that can have a varying spacing between 14 ft and 30 feet weigh 32 kip each.

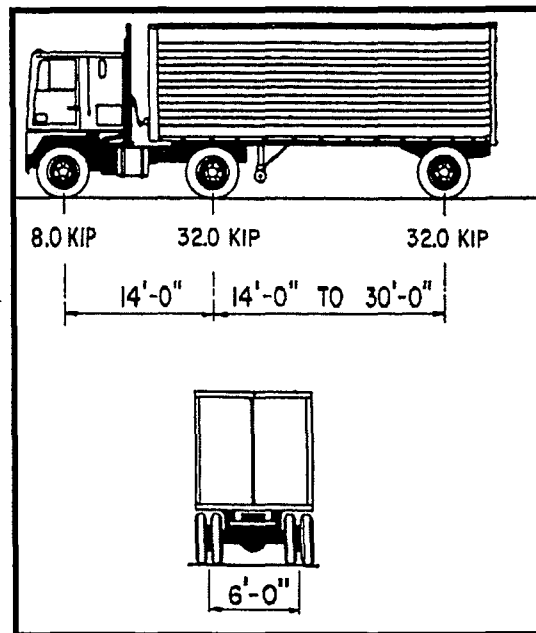


Figure 2.11: Characteristics of AASHTO LRFD Bridge Specification HS-20 truck

In order to produce the most force effect, the shortest spacing of 14 ft between the two rear axles is used in the computer model. Each axle load is distributed evenly between the two axle wheels. In other words, the two front wheels are each loaded with point loads of 4 kip and the four rear wheels are each loaded with point loads of 16 kip. Simplified wheel point loads are used to represent the loading. Although the load is more realistically distributed over the area of

contact between the wheel and the bridge deck, the simplification is necessary in order to more easily construct the computer model.

Transversely, the loading is placed in the center of the slow lane traveling in the northwest direction. The bridge width is 30' from curb to curb. Between the curbs are two 12' traffic lanes, both bounded by 3' shoulders. Therefore, the HS-20 truck is centered in the lane with 3' of space between the wheel load placements and the lane borders. This configuration is shown in Figure 2.12. Longitudinally, the HS-20 truck load is placed so that the center axle is directly above the chosen crack location. Therefore, the center axle of the truck is located at 77' from the south abutment where the flange thickness of the girder changes from 1-1/2" to 7/8".

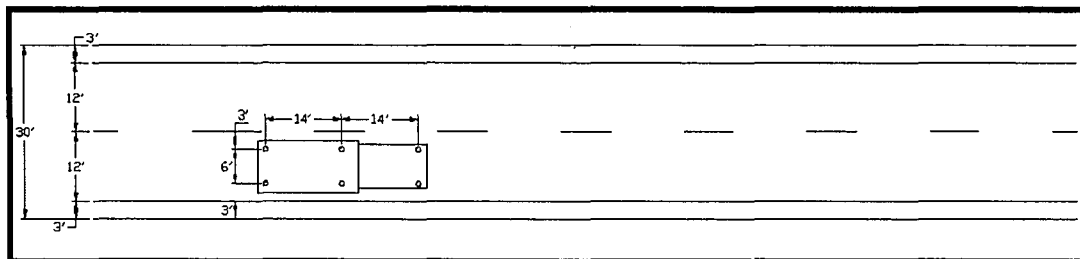


Figure 2.12: Lane and load configuration

2.6.3 Dynamic Loading

The two-girder two-span continuous bridge is analyzed to behave dynamically in two different conditions. The first analysis investigates the dynamic effect of the sudden release of the internal forces in both the flange crack (Stage 2) and the full depth crack (Stage 3). The second analysis studies the dynamic effect as an HS-20 truck load moves along the length of the bridge. The second dynamic effect is considered at Stage 1, 2, and 3 cracking.

The sudden crack release loading includes a statically placed HS-20 truck on the bridge. The HS-20 truck configuration is shown in Figure 2.11. The truck is again placed transversely in the center of the lane and longitudinally with the center axle of the truck directly in line with the crack cross section.

In order to simulate the sudden fracture of the girder, the analysis is done in two steps. For both Stage 2 and 3 cracking, the first analysis step is based on modeling the bridge as intact under dead and static live load. The second step for Stage 2 cracking is implemented by changing the boundary conditions of the cracked flange nodes. In simple terms, the unmerged cracked flange nodes are specified to displace the same amount as that between those computed for Stage 1 under the same loading conditions. For Stage 3 cracking, the unmerged cracked flange, web, and longitudinal stiffener nodes are specified to displace the same amount as that between those computed for Stage 1 under the same loading conditions. The entire first step is done statically, whereas the second analysis step involves the dynamic and sudden release of the crack. In the second analysis step the release of the crack is instantaneous, but the vibration or displacement of the bridge as a result of the crack release is analyzed at an interval of 0.01 seconds for a total time period of 0.2 seconds in order to capture the complete effect of the sudden release on the bridge behavior.

As stated, the second dynamic analysis studies the effect as an HS-20 truck load moving along the length of the bridge. The HS-20 truck is placed transversely in the center of the slow lane traveling in the northwest direction with the configuration shown in Figure 2.12. The truck is assumed to be moving at a speed of

61.36 mph (90 ft/s or 1080 in/s) which is a common speed for trucks over a two-girder bridge. The longitudinal movement of the truck's center axle is considered every 18 ft or 0.2 seconds. The truck placement is studied only over the span with the crack in the girder because of the long run-times involved in this dynamic analysis. Therefore, the first loading step is analyzed with the HS-20 center axle placed in line with the south abutment (only the front and center axles are on the bridge). The dynamic behavior of the two-girder bridge is examined at a time interval of 0.025 seconds for a time period of 0.2 seconds until the truck moves to its next location. The second loading step is analyzed with the HS-20 center axle placed at the same transverse direction as step 1, but at a longitudinal distance of 18 ft from the south abutment. The dynamic behavior of the bridge for the second loading step is examined at the same time interval of 0.025 seconds for a time period of 0.2 seconds (total time elapsed is 0.4 seconds). The truck movement and corresponding dynamic analysis is considered every 18 ft. The last loading step occurs when the HS-20 center axle is located at a longitudinal distance of 126 ft from the south abutment (just past the midspan longitudinal distance of 125 ft). The last load step occurs after 1.4 seconds of total time has elapsed, but the dynamic behavior of the bridge is examined for another 0.2 seconds.

The time interval of 0.025 seconds is selected in order to better capture the dynamic response to the moving truck load. Figure 2.13 illustrates the time variation of displacement for the G1 bottom flange to web connection of the intact bridge at a longitudinal distance of 56'-3" for two different time intervals. As shown from this

figure, the time interval of 0.05 seconds does not capture the full and maximum dynamic bridge response as does the time interval of 0.025 seconds.

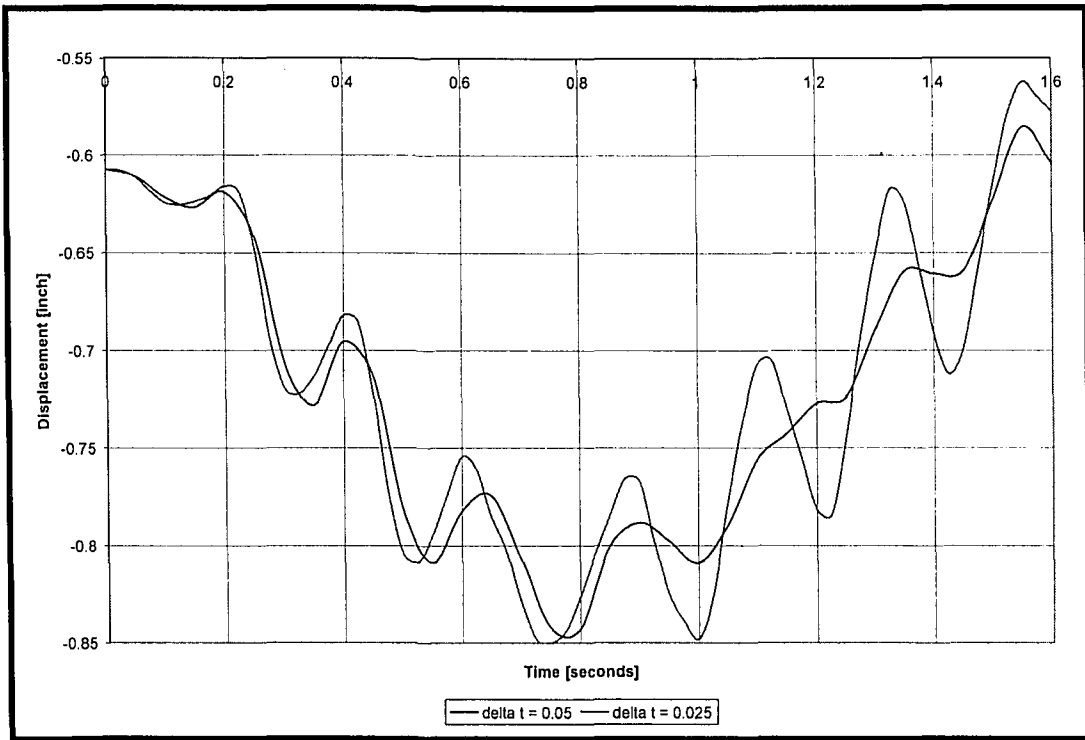


Figure 2.13: Time interval comparison for moving truck load

Chapter 3: Static Loading Analysis

3.1 Introduction

Static loading analysis is conducted to provide the basic and necessary information for the investigation of stress distribution and the possibility of drastic deflection after the crack develops. The static loading, especially under dead load only, also provides a base case for comparison between all the stages of cracking and later for a comparison against dynamic loading. Lastly, the static loading cases illustrate critical locations where steel may be yielding or concrete may be crushing and where deflection is maximum. Each cracking stage is analyzed under static dead load as well as under both static dead and live load. Dead load analysis is only discussed in detail for Stage 1, but will be used for comparison later.

3.2 Stage 1

Stage 1 static loading analysis examines the two-girder two-span continuous bridge intact with dead load and the HS-20 truck placed with its center axle above the crack cross section location.

3.2.1 Stage 1 Dead Load Analysis

Analyzing the intact two-girder two-span continuous bridge under dead load illustrates the symmetric nature of the bridge about both the centerline of the bridge as well as about the center support. The symmetry between the spans as well as the overall vertical deflection shape of the bridge due to dead load is shown in Figure

3.1. The deflection shown is in actual scale, but is in much larger scale with respect to the lengths of the bridge.

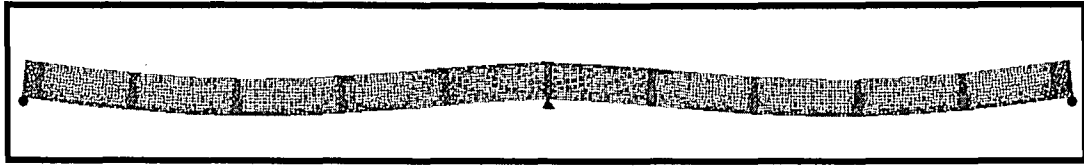


Figure 3.1: Stage 1 deflection due to dead load

Maximum overall vertical deflection (0.66") of the intact bridge under dead load is located in the deck between FB3 and mid-span (see Appendix A for bridge plans and labeling) at about 57 ft from the abutment. Figure 3.2 shows the contour of vertical deflection of one span of the two-girder two-span continuous bridge steel superstructure. As seen in the figure, the deflection contours are continuous. Along the transverse direction of the bridge the vertical deflection is all about the same magnitude at any bridge cross section. The vertical deflection of the girders at a longitudinal distance of 56'-3" is 0.6073".

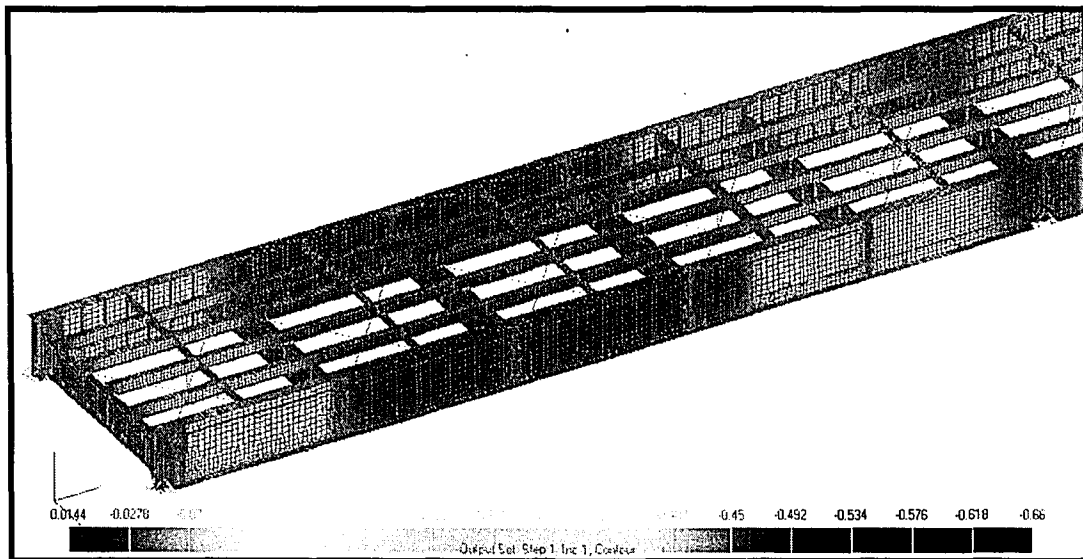


Figure 3.2: Stage 1 contoured vertical deflection due to dead load

3.1. The deflection shown is in actual scale, but is in much larger scale with respect to the lengths of the bridge.

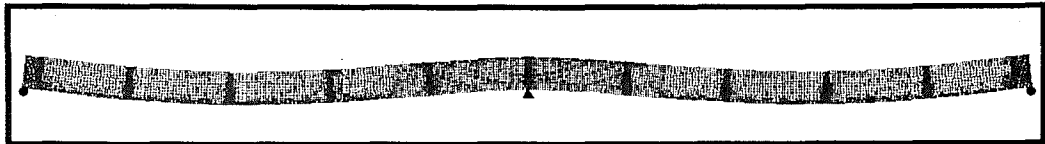


Figure 3.1: Stage 1 deflection due to dead load

Maximum overall vertical deflection (0.66") of the intact bridge under dead load is located in the deck between FB3 and mid-span (see Appendix A for bridge plans and labeling) at about 57 ft from the abutment. Figure 3.2 shows the contour of vertical deflection of one span of the two-girder two-span continuous bridge steel superstructure. As seen in the figure, the deflection contours are continuous. Along the transverse direction of the bridge the vertical deflection is all about the same magnitude at any bridge cross section. The vertical deflection of the girders at a longitudinal distance of 56'-3" is 0.6073".

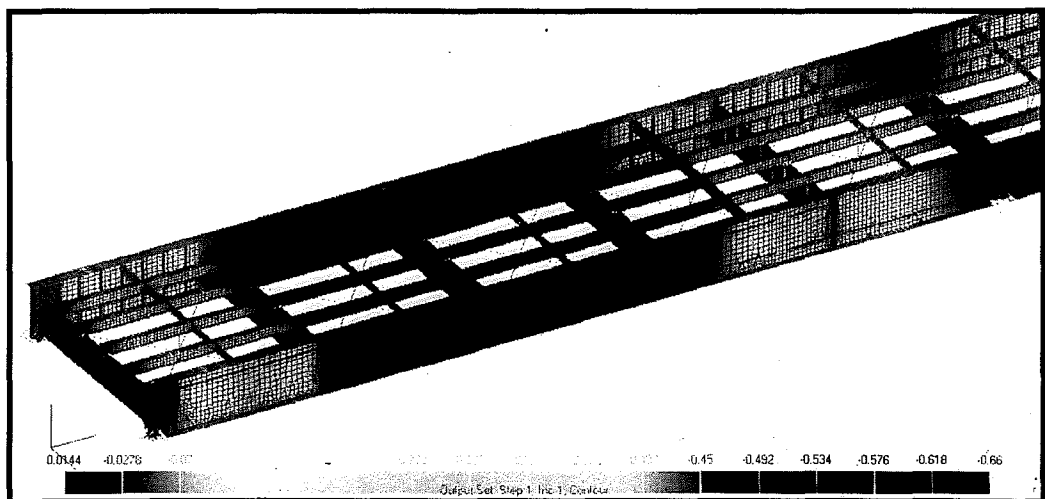


Figure 3.2: Stage 1 contoured vertical deflection due to dead load

Stress levels for the intact bridge under dead load are generally low except at certain locations where there is local stress concentration. The three main locations where there are localized stress concentrations are at the mid-support (Pier 1), at the lateral bracing member to gusset plate connection, and at the floorbeam top flange connection to the girder. Because the purpose of the preliminary project is to focus on the behavior and redundancy of the bridge structure, not on these localized stress locations away from the cracked cross section, simplifications are adopted in the model. The lateral bracing member is connected to the gusset plate at one node, instead of at multiple locations along the plate. The bearing at all supports is modeled as a line of constraints, instead of an area of constraints. The transition radius at the floorbeam top flange to girder connection is omitted. The higher stress values at these localized locations are ignored unless the high stress starts to spread.

On the global level, the maximum stress in the intact bridge under dead load is not greater than 10 ksi. Maximum stress is located in the two girders. This is due to the fact that the girders are the main load carrying members of the bridge. The stress contour of normal stresses (tension and compression) in one span of the girder is shown in Figure 3.3.

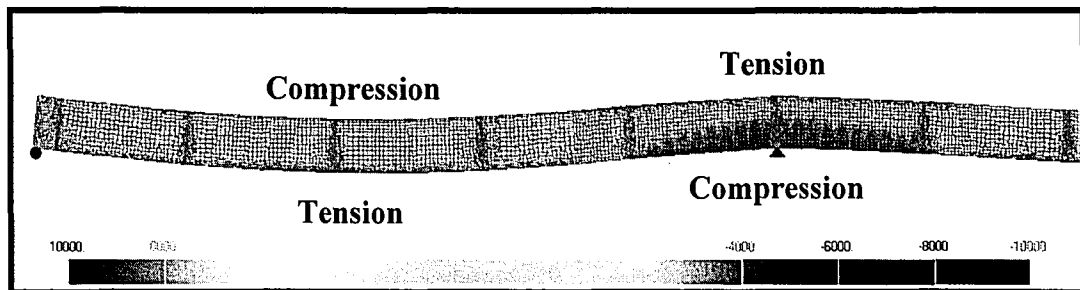


Figure 3.3: Stress contour in Stage 1 under dead load

Stress levels for the intact bridge under dead load are generally low except at certain locations where there is local stress concentration. The three main locations where there are localized stress concentrations are at the mid-support (Pier 1), at the lateral bracing member to gusset plate connection, and at the floorbeam top flange connection to the girder. Because the purpose of the preliminary project is to focus on the behavior and redundancy of the bridge structure, not on these localized stress locations away from the cracked cross section, simplifications are adopted in the model. The lateral bracing member is connected to the gusset plate at one node, instead of at multiple locations along the plate. The bearing at all supports is modeled as a line of constraints, instead of an area of constraints. The transition radius at the floorbeam top flange to girder connection is omitted. The higher stress values at these localized locations are ignored unless the high stress starts to spread.

On the global level, the maximum stress in the intact bridge under dead load is not greater than 10 ksi. Maximum stress is located in the two girders. This is due to the fact that the girders are the main load carrying members of the bridge. The stress contour of normal stresses (tension and compression) in one span of the girder is shown in Figure 3.3.

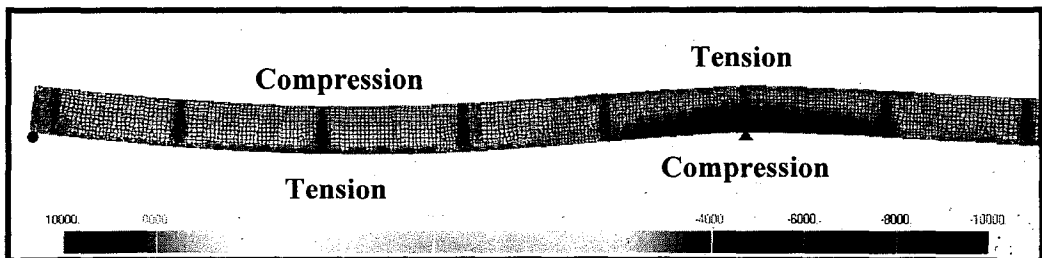


Figure 3.3: Stress contour in Stage 1 under dead load

3.2.2 Stage 1 Dead and Live Load Analysis

The maximum overall vertical deflection (0.88") of the intact two-girder two-span continuous bridge under both dead and live load is located in the mid-span diaphragm connection to S2. This deflection is an increase of about 33% compared to that of dead load alone. Obviously, the 72 kips of live load of the HS-20 truck causes proportionally much more deflection near the live load. The maximum vertical deflection in the adjacent span is reduced from 0.66" under dead load alone to about 0.6" with the addition of live load. Figure 3.4 depicts the deflection shape of the girder when the bridge is under the addition of live load.

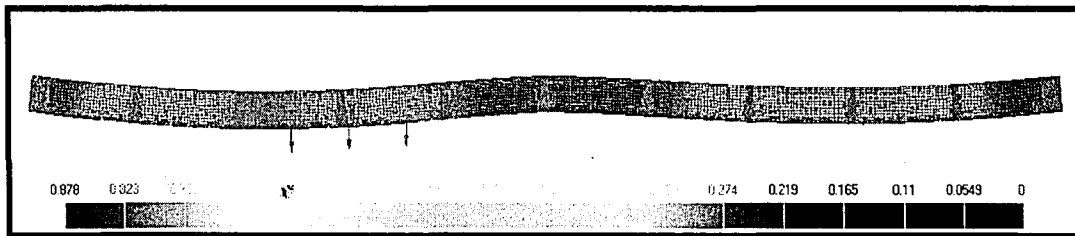


Figure 3.4: Stage 1 girder deflection due to dead and live load

Figure 3.5 compares the dead load and dead plus live load deflection in the girder closest to the HS-20 truck. The location of maximum girder deflection for dead and live load shift slightly from that for dead load alone due to the placement of the live load. With the addition of live load, the stringers and diaphragm under the truck are deflecting more. This deflection is illustrated in Figure 3.6 with an exaggerated scale.

3.2.2 Stage 1 Dead and Live Load Analysis

The maximum overall vertical deflection (0.88") of the intact two-girder two-span continuous bridge under both dead and live load is located in the mid-span diaphragm connection to S2. This deflection is an increase of about 33% compared to that of dead load alone. Obviously, the 72 kips of live load of the HS-20 truck causes proportionally much more deflection near the live load. The maximum vertical deflection in the adjacent span is reduced from 0.66" under dead load alone to about 0.6" with the addition of live load. Figure 3.4 depicts the deflection shape of the girder when the bridge is under the addition of live load.

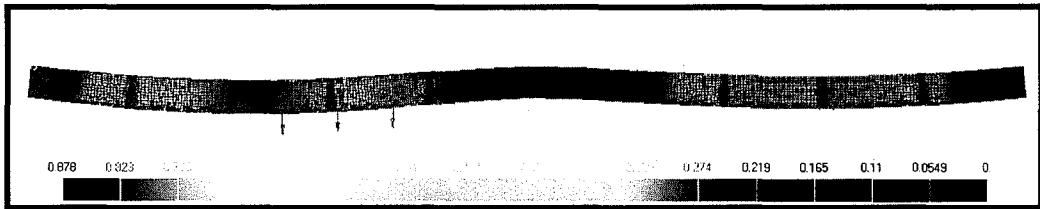


Figure 3.4: Stage 1 girder deflection due to dead and live load

Figure 3.5 compares the dead load and dead plus live load deflection in the girder closest to the HS-20 truck. The location of maximum girder deflection for dead and live load shift slightly from that for dead load alone due to the placement of the live load. With the addition of live load, the stringers and diaphragm under the truck are deflecting more. This deflection is illustrated in Figure 3.6 with an exaggerated scale.

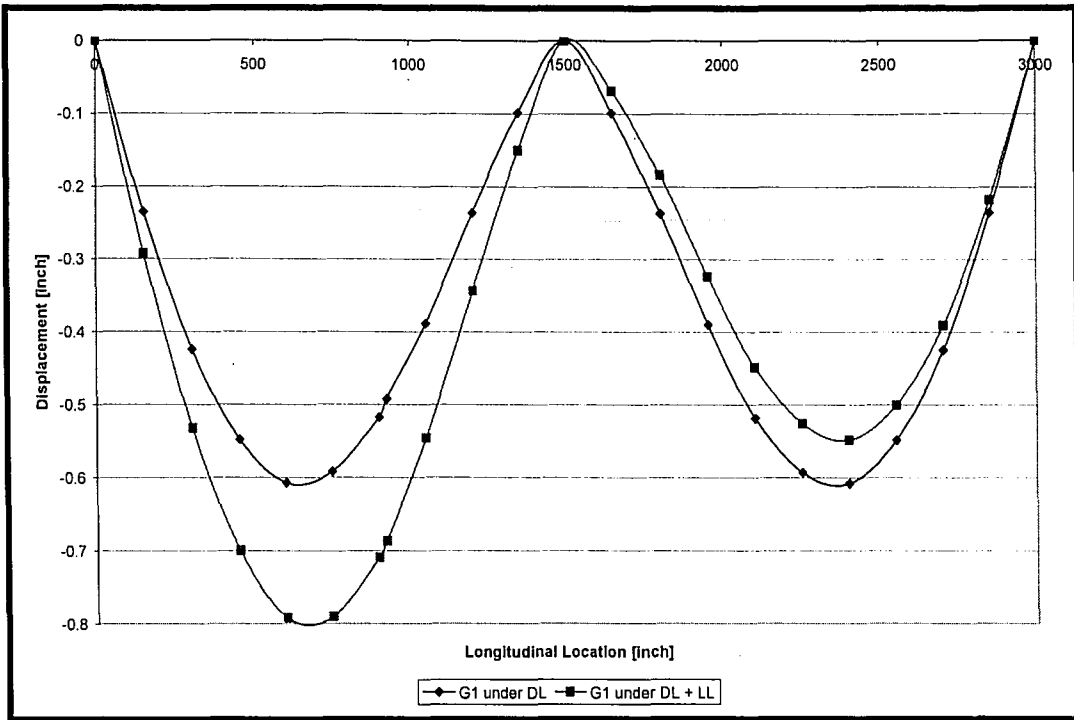


Figure 3.5: Stage 1 G1 dead load deflection versus dead and live load deflection

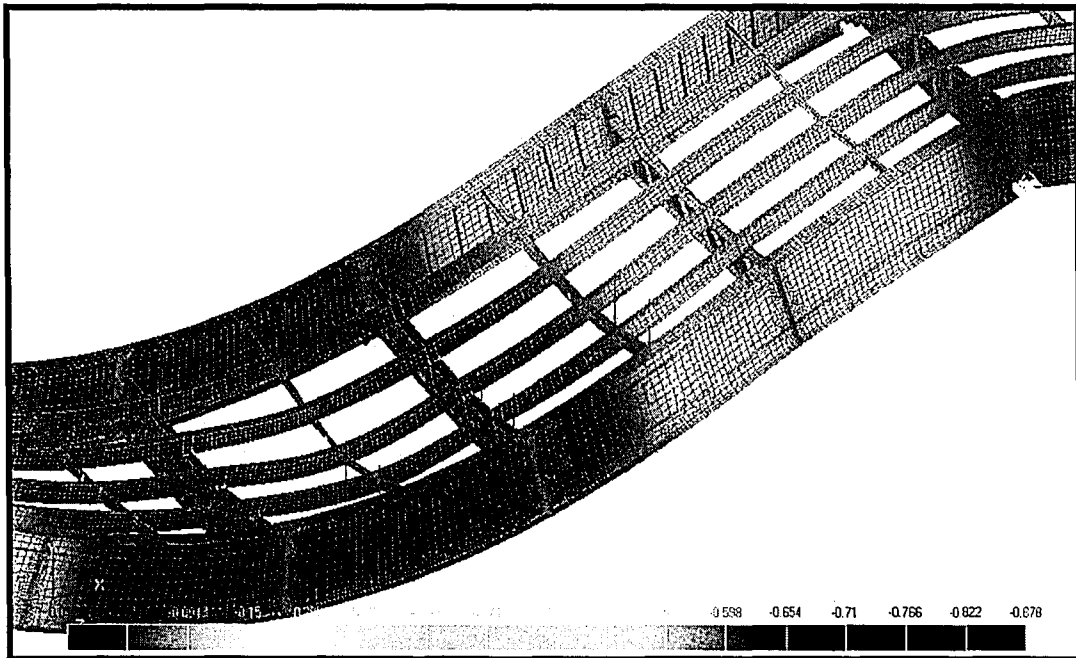


Figure 3.6: Stage 1 stringer and diaphragm deflection due to dead and live load

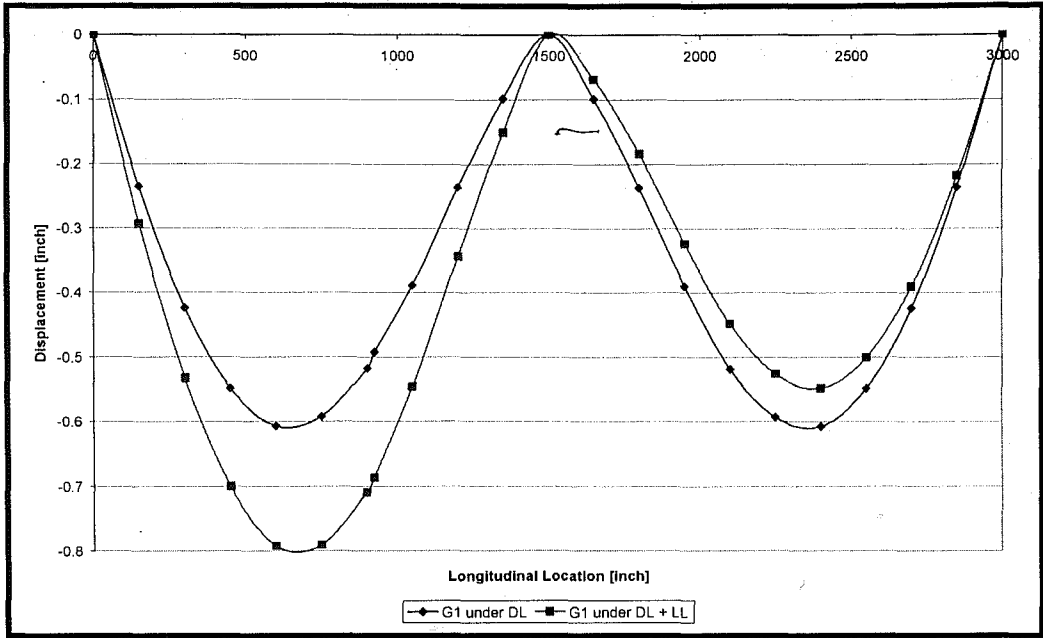


Figure 3.5: Stage 1 G1 dead load deflection versus dead and live load deflection

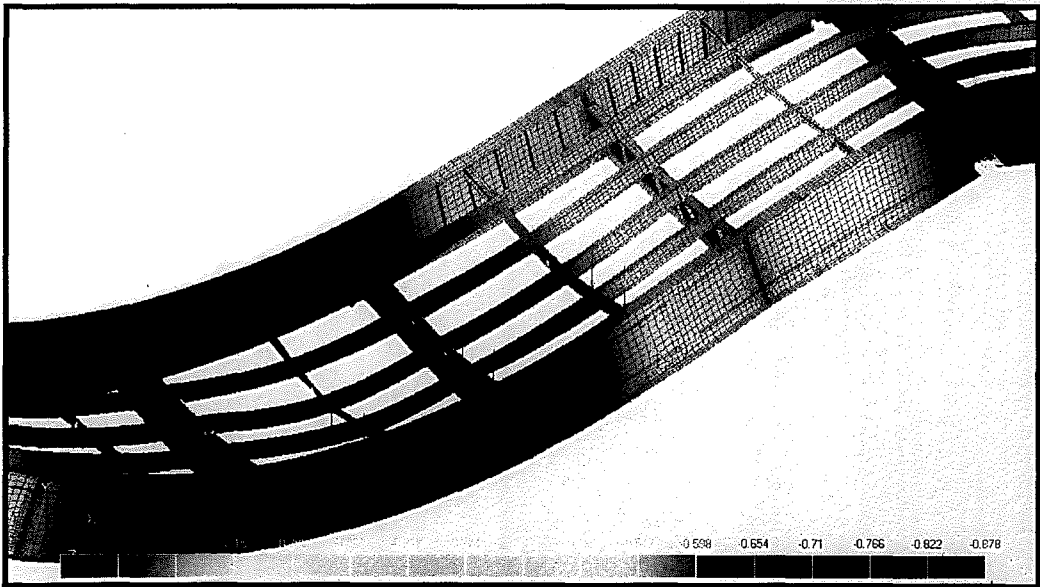


Figure 3.6: Stage 1 stringer and diaphragm deflection due to dead and live load

The magnitude of stresses with the addition of live load at Stage 1 does not change appreciably as compared to those due to dead load alone. As mentioned in section 3.2.1, localized stresses due to modeling of details are ignored. There is no globalized yielding in any of the steel components and the stresses in the concrete deck are all below limit.

The maximum stress is located in the girder close to the HS-20 truck loading (the girder of imposed crack later). Maximum stress (about 10 ksi in tension) is in the bottom flange of the girder near the connection to FB3. The maximum stress in the thinner flange plate, about 20 ft away at the transition thickness in the tension flange, is about 9 ksi. The stress contour at the change in flange thickness is illustrated in Figure 3.7. The maximum stress in G1 is 9.79 ksi, in G2 is 9.52 ksi, in the lateral bracings is 4.41 ksi, in the floorbeams is 3.39 ksi, and in the stringers and diaphragms is 12.07 ksi.

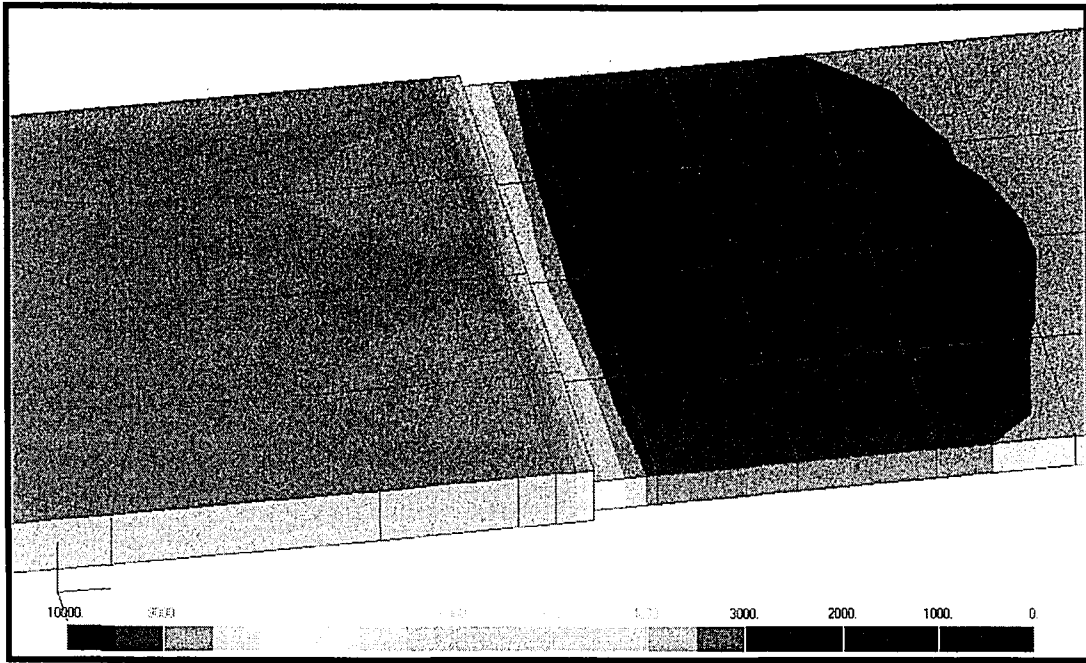


Figure 3.7: Stage 1 stresses at change in flange thickness due to dead and live load

3.3 Stage 2

Stage 2 static loading analysis examines the two-girder two-span continuous bridge with the tension flange of one girder cracked and an HS-20 truck placed with its center axle above the crack cross section location.

3.3.1 Displacement

The existence of the flange crack does not significantly change the amount of deflection anywhere along the length of the bridge as compared to the intact bridge. The maximum overall vertical deflection only increases from 0.88" to about 0.89", which is a 1.1% increase. The location of maximum deflection in the two-girder two-span continuous bridge, as in Stage 1 under dead and live load, is still at the mid-span diaphragm to S2 connection. Maximum deflection in the girders is

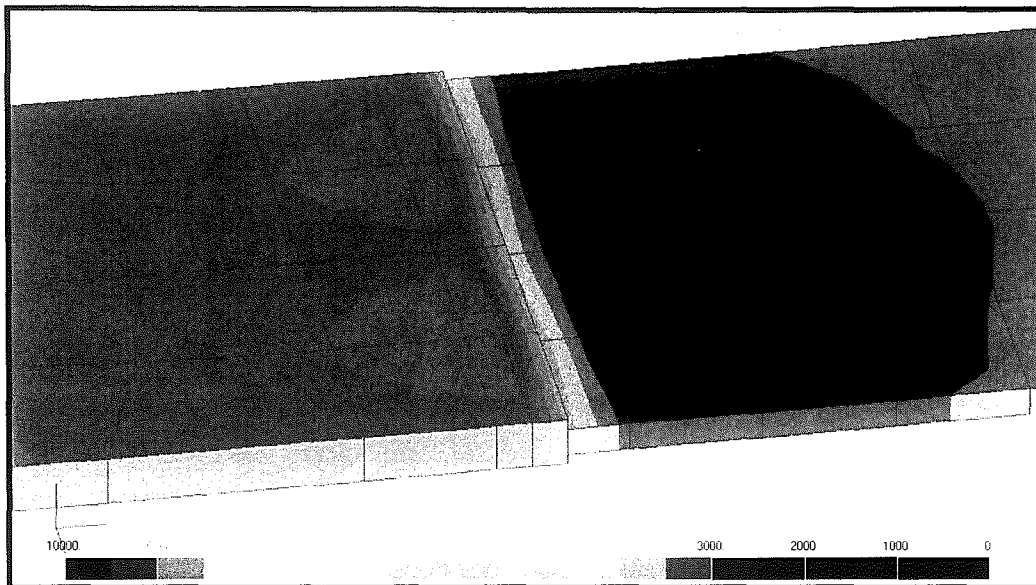


Figure 3.7: Stage 1 stresses at change in flange thickness due to dead and live load

3.3 Stage 2

Stage 2 static loading analysis examines the two-girder two-span continuous bridge with the tension flange of one girder cracked and an HS-20 truck placed with its center axle above the crack cross section location.

3.3.1 Displacement

The existence of the flange crack does not significantly change the amount of deflection anywhere along the length of the bridge as compared to the intact bridge. The maximum overall vertical deflection only increases from 0.88" to about 0.89", which is a 1.1% increase. The location of maximum deflection in the two-girder two-span continuous bridge, as in Stage 1 under dead and live load, is still at the mid-span diaphragm to S2 connection. Maximum deflection in the girders is

0.8095". Figure 3.8 illustrates the deflection comparison between Stage 1 and 2 under dead and live load for the cracked girder.

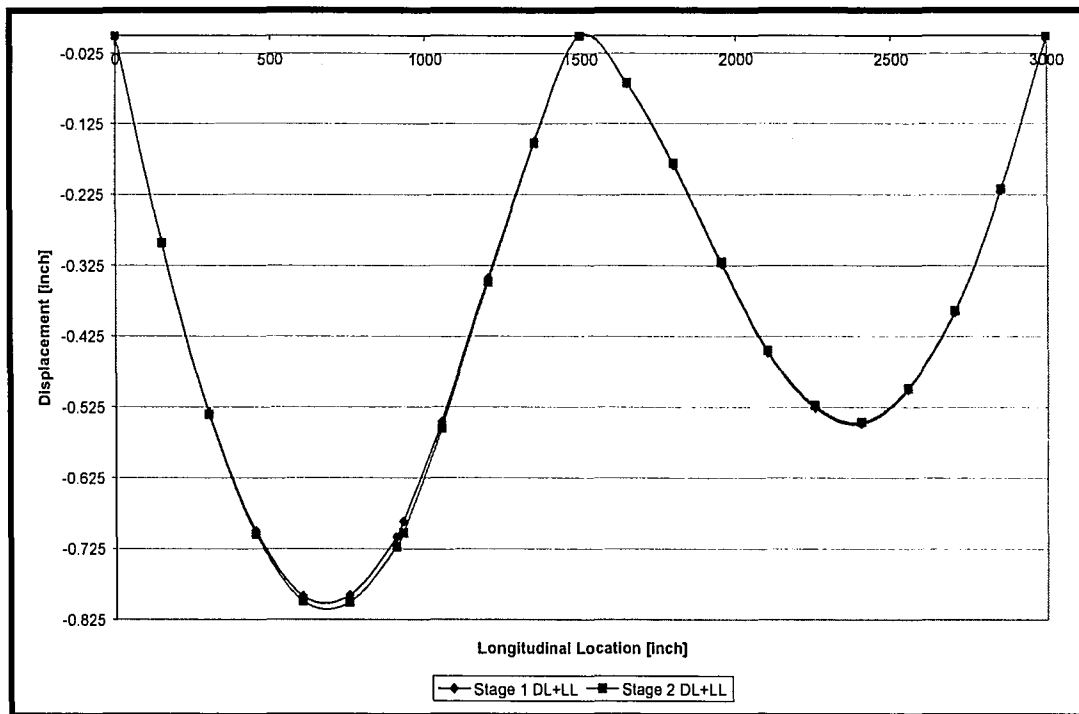


Figure 3.8: G1 displacement comparison between Stage 1 and Stage 2 under dead and live load

As shown by Figure 3.8, the deflection of Stage 2 is almost exactly in line with Stage 1. The only noticeable difference is that Stage 2 deflects slightly more in the first span at the maximum girder deflection location. This insignificant change in deflection between Stage 1 and Stage 2 suggests that the two-girder two-span continuous bridge could continue in-service with a flange crack in the girder.

3.3.2 Stress

With the existence of a flange crack, localized high stresses develop. Figure 3.9 shows the stress contour near the crack tip. The highest magnitude by the finite element analysis is about 41 ksi near the crack tip. Away from the crack, the stress

distribution along the bridge is almost unchanged between Stage 1 and Stage 2. The maximum stress in G1 is 9.71 ksi, in G2 is 9.55 ksi, in the lateral bracings is 4.36 ksi, in the floorbeams is 3.37 ksi, and in the stringers and diaphragms is 12.12 ksi.

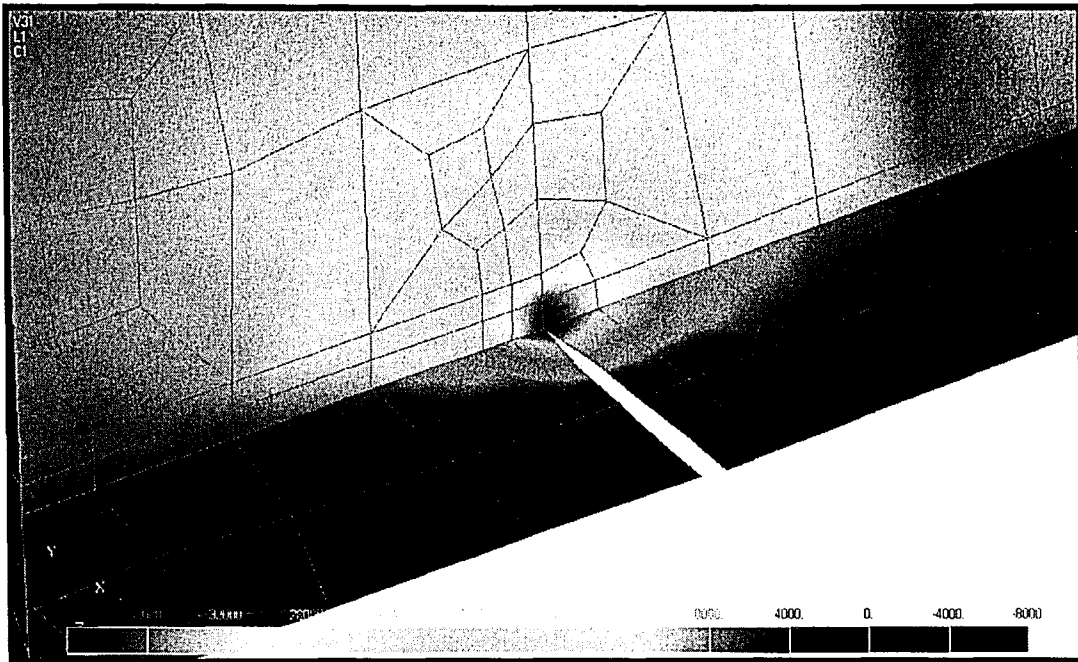


Figure 3.9: Stress near the crack at Stage 2

The condition of only minor changes in stress distribution and displacement indicates that the two-girder two-span continuous bridge retains its normal behavior. The crack can continue to service even with a flange crack in the girder.

3.4 Stage 3

Stage 3 static loading analysis examines the two-girder two-span continuous bridge with a full depth crack to the top of the girder web and an HS-20 truck placed with its center axle above the crack cross section location.

distribution along the bridge is almost unchanged between Stage 1 and Stage 2. The maximum stress in G1 is 9.71 ksi, in G2 is 9.55 ksi, in the lateral bracings is 4.36 ksi, in the floorbeams is 3.37 ksi, and in the stringers and diaphragms is 12.12 ksi.

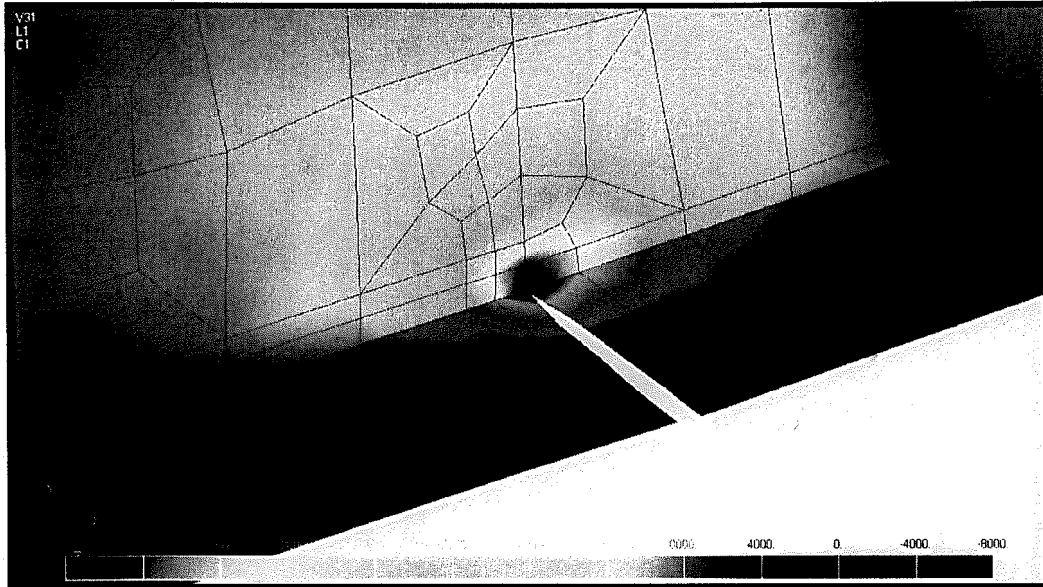


Figure 3.9: Stress near the crack at Stage 2

The condition of only minor changes in stress distribution and displacement indicates that the two-girder two-span continuous bridge retains its normal behavior. The crack can continue to service even with a flange crack in the girder.

3.4 Stage 3

Stage 3 static loading analysis examines the two-girder two-span continuous bridge with a full depth crack to the top of the girder web and an HS-20 truck placed with its center axle above the crack cross section location.

3.4.1 Displacement

The full depth crack to the top of the girder web increases the overall displacement of the bridge drastically. Figure 3.10 is an overall image of the southern span of the two-girder two-span continuous bridge with a full depth crack (Stage 3). The maximum deflection is about 1.22" at the crack location. The girder and bridge deflection is different on either side of the crack and the maximum deflection is located on the southern portion of the span. The cross section of the girder on the other side of the crack deflects (1.19") appreciably less because of the support provided by the uncracked northern span.

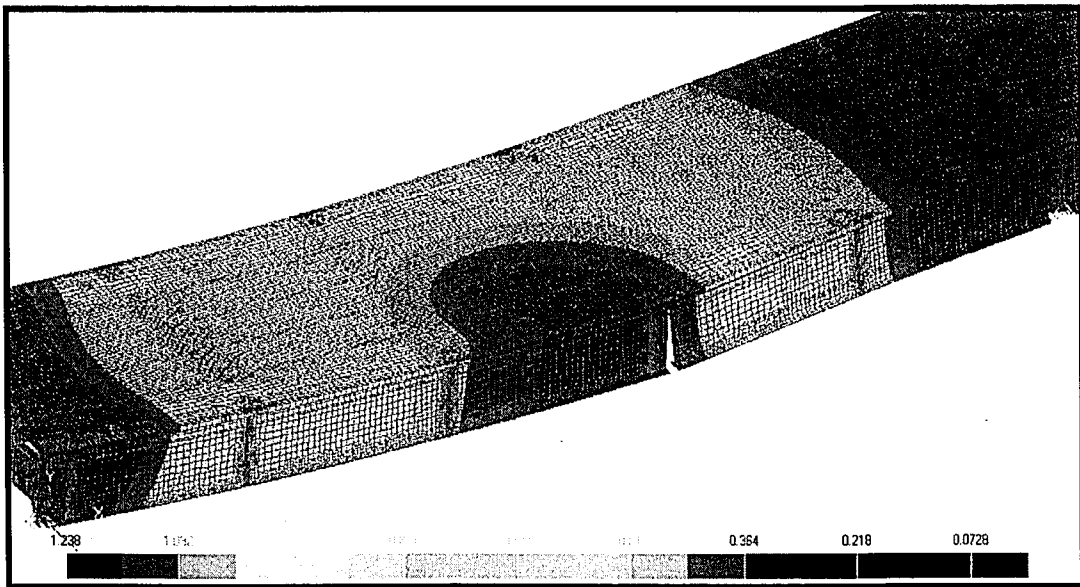


Figure 3.10: Deflection contours under Stage 3 cracking with dead and live load

Unlike with Stage 1 and 2 deflections of the girder, the change in magnitude of deflection to the Stage 3 crack is much more significant (about 45% increase). The deflected shape also changes because the crack has such a large effect. Figure

3.4.1 Displacement

The full depth crack to the top of the girder web increases the overall displacement of the bridge drastically. Figure 3.10 is an overall image of the southern span of the two-girder two-span continuous bridge with a full depth crack (Stage 3). The maximum deflection is about 1.22" at the crack location. The girder and bridge deflection is different on either side of the crack and the maximum deflection is located on the southern portion of the span. The cross section of the girder on the other side of the crack deflects (1.19") appreciably less because of the support provided by the uncracked northern span.

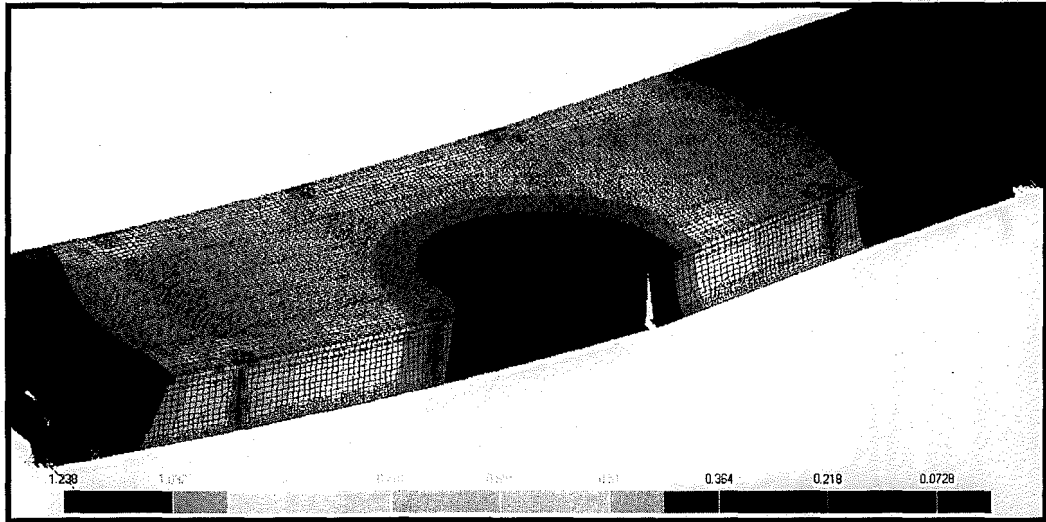


Figure 3.10: Deflection contours under Stage 3 cracking with dead and live load

Unlike with Stage 1 and 2 deflections of the girder, the change in magnitude of deflection to the Stage 3 crack is much more significant (about 45% increase). The deflected shape also changes because the crack has such a large effect. Figure

3.11 illustrates the deflection comparison between Stage 1, Stage 2, and Stage 3 cracking in G1.

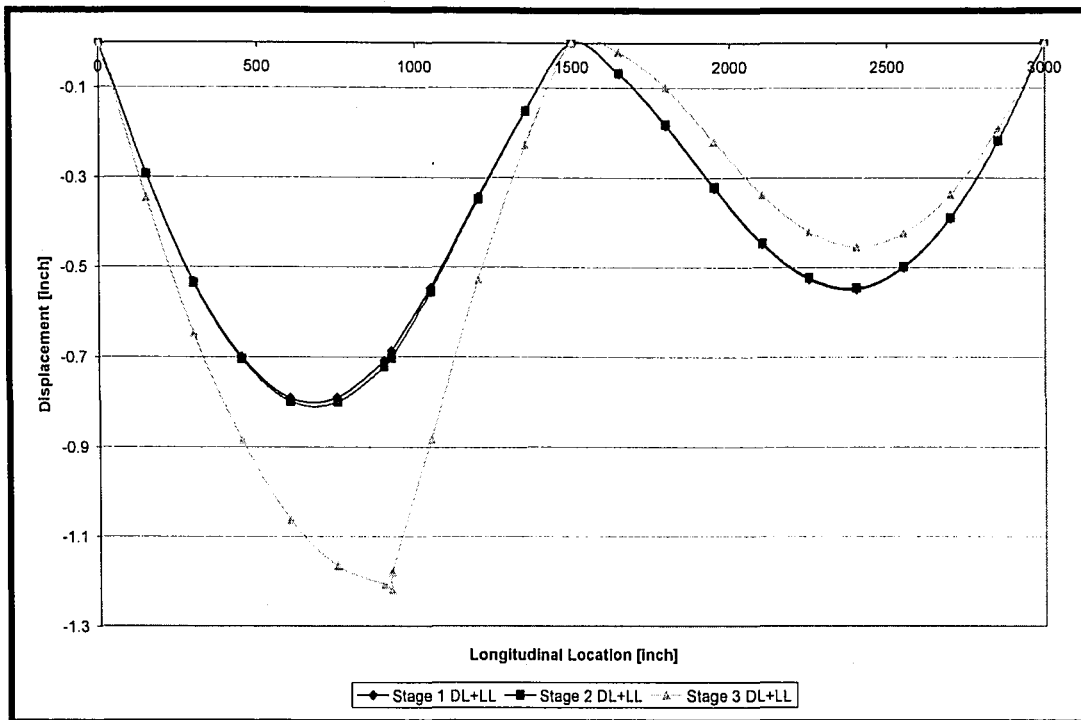


Figure 3.11: G1 displacement comparison between Stage 1, 2, and 3 under dead and live load

Despite the larger deflections under Stage 3 cracking as compared to Stage 1 and Stage 2, the maximum deflection is only 1.22". This is not such a large deflection for a bridge span of 125 ft and probably not noticeable on the bridge deck if the deck has not failed. The two-girder two-span continuous bridge remains standing without collapsing.

3.4.2 Stress

Even with the full depth crack in the girder web, nowhere in the steel superstructure is there any yielding. The maximum stress in G1 is 18.5 ksi, in G2 is 10.5 ksi, in the lateral bracings is 7.68 ksi, in the floorbeams is 6.18 ksi, and in the stringers and diaphragms is 13.58 ksi. The crack tip is no longer experiencing such a

concentration of localized stress as it was for Stage 2. However, the deflection of the concrete deck is large enough to cause a region (approximately 13 sq. ft) with tension stresses higher than the specified tensile limit of 0.4 ksi. Figure 3.12 illustrates the tension region. The compressive stress in the concrete is below the specified strength limit of 3.5 ksi. Therefore, there are no regions where the concrete is crushing.

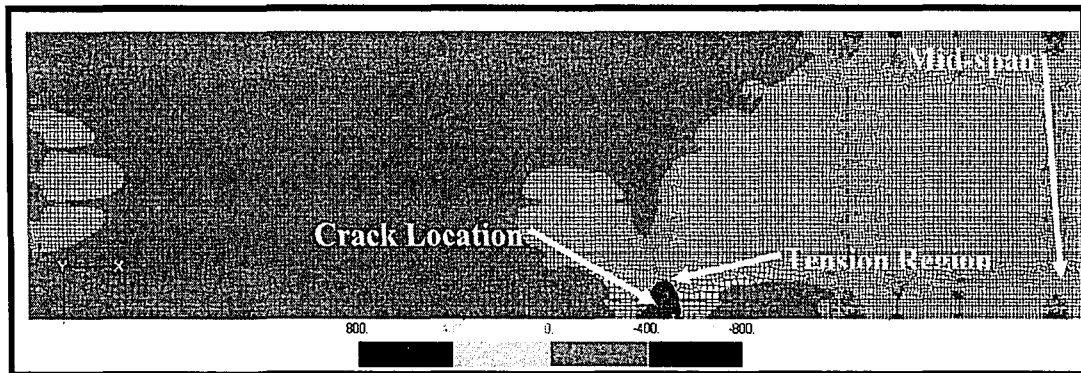


Figure 3.12: Concrete region failing for Stage 3 cracking under static dead and live load

It is noted that, as a conservative approximation, the concrete deck is not modeled with any steel reinforcement. If the deck were modeled with steel reinforcement, the region of tensile stress would be much smaller.

Chapter 4: Dynamic Loading Analysis

4.1 Introduction

Dynamic loading analysis is conducted to provide a more realistic estimate as to how the bridge behaves under actual loading conditions. As with the static loading analysis, the possibility of drastic deflection after crack development and the corresponding stress distribution are examined. The two-girder two-span continuous bridge is analyzed under two dynamic conditions. The first condition is the sudden dynamic release of the crack with a static HS-20 truck live load placed with its center axle directly above the crack cross section. The second condition is the dynamic effect on the bridge from a moving HS-20 truck live load. The condition of sudden dynamic release of a crack with a moving HS-20 truck is a more serious case. However, the process for direct computation is beyond the capacity of this preliminary study. A method for approximation is presented in Chapter 6 later.

4.2 Sudden Release of Crack

The dynamic analysis of the sudden release of a crack provides an accurate portrayal of how the two-girder two-span continuous bridge responds to a sudden fracture of a component of the bridge. The sudden release of a crack (by displacement) simulates the fracture. Since the bridge structure is subjected to larger deflection and higher stress under live load, the static HS-20 truck live load is placed on the bridge as described in Section 2.6.2 to produce the worst case scenario for the fracture to occur. The crack is released suddenly for both Stage 2 and Stage 3 cracking and the dynamic bridge response is examined accordingly.

4.2.1 Stage 2 Crack Release Dynamic Response

The crack release is sudden or instantaneous. The dynamic response of the bridge is analyzed every 0.01 seconds for a total time of 0.2 seconds. This time frame does not capture the entire dynamic effect of the crack release. However, it does encapsulate the points of maximum deflection and maximum stress.

It is known from the static analysis of Stage 2 that the maximum displacement of the girder is located at a longitudinal distance of 56'-3" from the southern abutment. Therefore, the displacement of the two-girder two-span continuous bridge is analyzed in close proximity to that longitudinal distance. This is done in order to find out at what time the maximum displacement occurs. Figure 4.1 illustrates the deflection profile of the girder near the point of maximum displacement for all time increments of Stage 2.

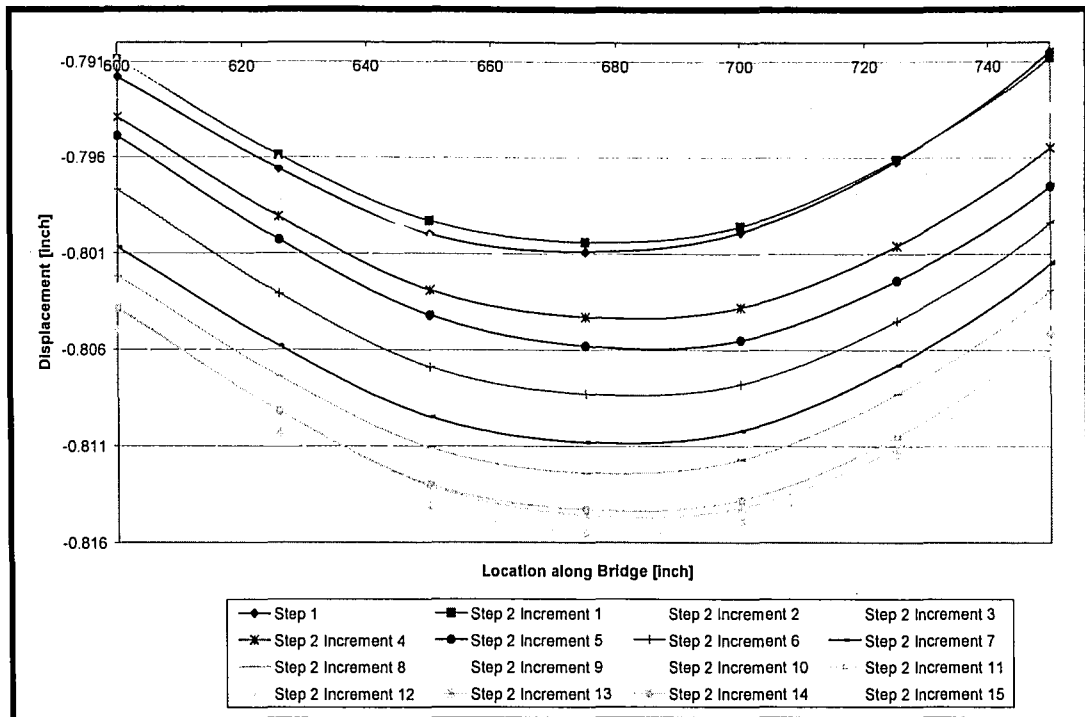


Figure 4.1: Displacement response to the dynamic release of crack at all Stage 2 time increments

Figure 4.1 shows that the deflection of the girder continues to increase after step 1 (static dead load condition) until it reaches time increment 11 (0.11 seconds) when maximum deflection occurs. After this time, the bridge deflection reduces due to the decreasing amplitude of vibration response. The time variation of deflection (at 56'-3" from the southern abutment) at the point of maximum deflection is shown in Figure 4.2. This location is a reference point only for maximum static deflection.

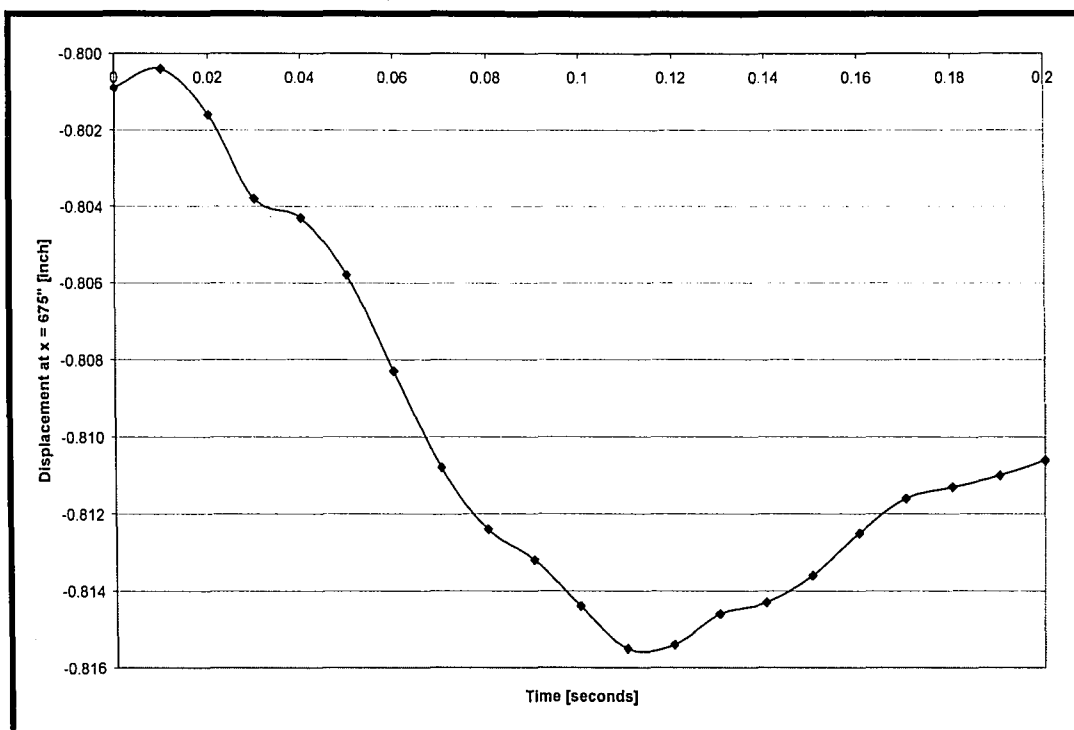


Figure 4.2: Maximum dynamic displacement response to Stage 2 crack release varying with time

In Figure 4.2, the displacement at zero time is the maximum value at Step 1 of Figure 4.1, which is the same as Stage 1 under dead and static live load. The magnitude of deflection at this step or time is 0.8009". The deflection at this location increases to a highest magnitude of 0.8155" at 0.11 seconds of dynamic response. This is only an increase of 0.0146" from the static loading of Stage 1 (about a 2% increase). Including the dynamic response of the bridge, due to the sudden fracture of Stage 2, results in a magnitude of deflection larger than that of the static release of the flange crack (0.8155" versus 0.8095", an increase of less than 1%).

Figure 4.3 further illustrates the small difference when comparing the dynamic fracture to the static crack opening of the flange crack. This suggests that

incorporating the crack in a static analysis can predict the girder deflection for small cracks. Also, the small deflection from the sudden fracture of the flange suggests that the two-girder two-span continuous bridge can continue to be in service with the flange crack.

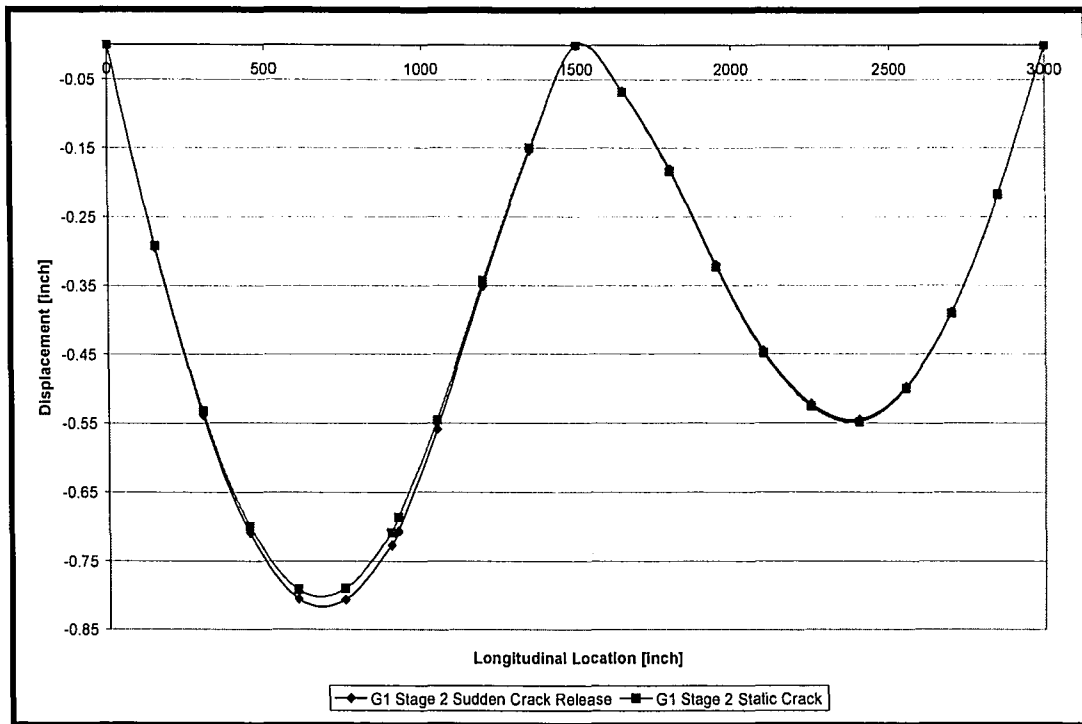


Figure 4.3: Stage 2 sudden crack release displacement versus Stage 2 static crack displacement

The stress distribution for the sudden crack release in Stage 2 is essentially the same as the stress distribution for the static crack release. The web plate at the flange crack is experiencing localized stresses as illustrated in Figure 3.9. However, there is no yielding of any steel component or any concrete failing. The maximum stress in G1 is 9.75 ksi, in G2 is 9.61 ksi, in the lateral bracings is 4.37 ksi, in the floorbeams is 3.41ksi, and in the stringers and diaphragms is 12.19 ksi. This

situation reinforces the suggestion that the bridge will not collapse under the dynamic fracture of the flange with a static HS-20 truck on the bridge.

4.2.2 Stage 3 Crack Release Dynamic Response

The Stage 3 crack release is instantaneous and the dynamic response of the bridge is analyzed every 0.01 seconds for a total time of 0.21 seconds. As in Stage 2, this chosen time frame does not capture the entire dynamic effect of the crack release, but does encapsulate the points of maximum deflection and maximum stress.

It is known from the static analysis of Stage 3 that the maximum displacement of the girder is located at the southern face of the crack. Therefore, the displacement of the two-girder two-span continuous bridge is examined in the close proximity. This reveals at what time the maximum displacement occurs. The deflection profiles of the girder flange near the crack for all time increments of Stage 3 are shown in Figure 4.4.

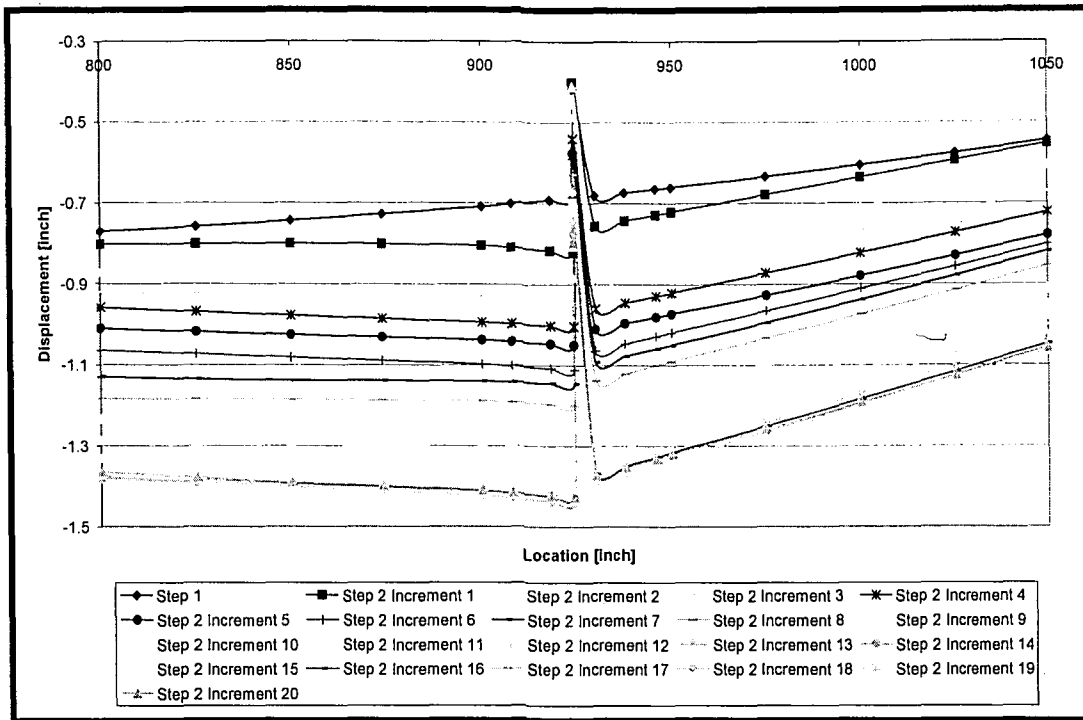


Figure 4.4: Displacement response to the dynamic release of crack at all Stage 3 time increments

The deflection profiles in Figure 4.4 depict the large difference between the two sides of the crack as well as an overall picture of the bridge response. However, it is difficult to distinguish the increment of displacement with time at the maximum deflection. Figure 4.5 focuses on the maximum deflection of the girder closer to the crack at time increments approaching the maximum. The maximum deflection is computed to be 1.4437" at 0.18 seconds (increment 18). After 0.18 seconds, the deflection begins to decrease due to the vibrational characteristics of the bridge.

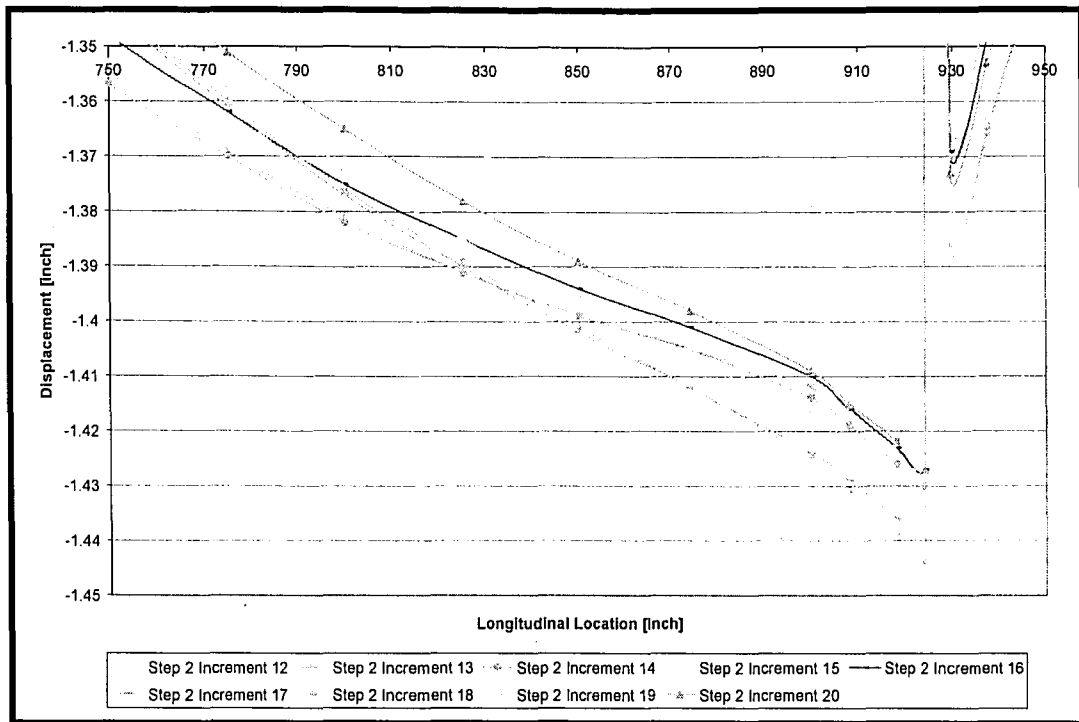


Figure 4.5: Maximum dynamic displacement response to the release of Stage 3 at selected time increments

Figure 4.5 also shows that the time where points of the bridge attain their respective maximum deflection is not the same along the length of the bridge. This study concentrates on the maximum deflection at the crack and the redundancy of the bridge. The maximum deflection at the crack is shown in Figure 4.6 as it varies with time.

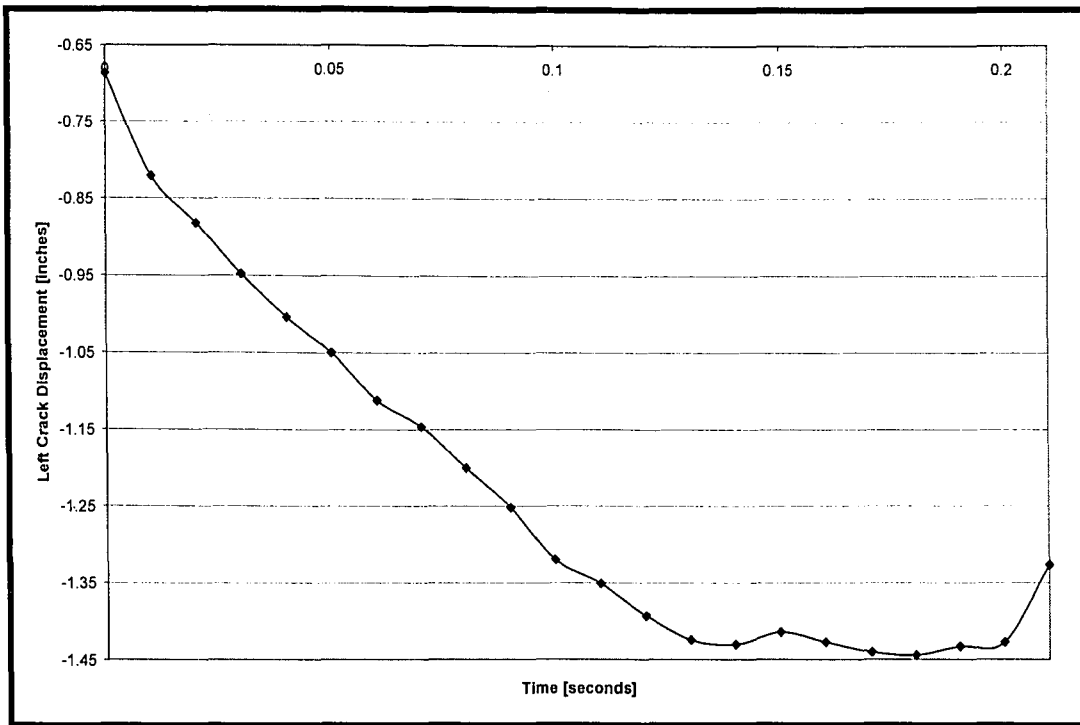


Figure 4.6: Maximum dynamic displacement response to Stage 3 crack release varying with time

In Figure 4.6, the crack displacement at zero time is the same that at as Stage 1 under dead and static live load. The deflection at this step is 0.6867". The deflection increases to a maximum of 1.4437" at 0.18 seconds of dynamic response. This is an increase of 0.757" from the static loading of Stage 1 (about 110%). The corresponding deflection by the static release of the full depth crack (Stage 3) is 1.2186". So, the sudden fracture of Stage 3 increases the deflection by about 18% compared to the static release of the full-depth crack.

This relatively large difference between deflection due to dynamic fracture and static crack opening is revealed in Figure 4.7. It is interesting to observe that the dynamic deflection in the adjacent span without live load is less than that by static crack opening. Despite the relatively large deflection under the sudden dynamic release of the full depth crack, the girder remains stable and the two-girder two-span

continuous bridge does not collapse. This condition implies redundancy of the bridge structure.

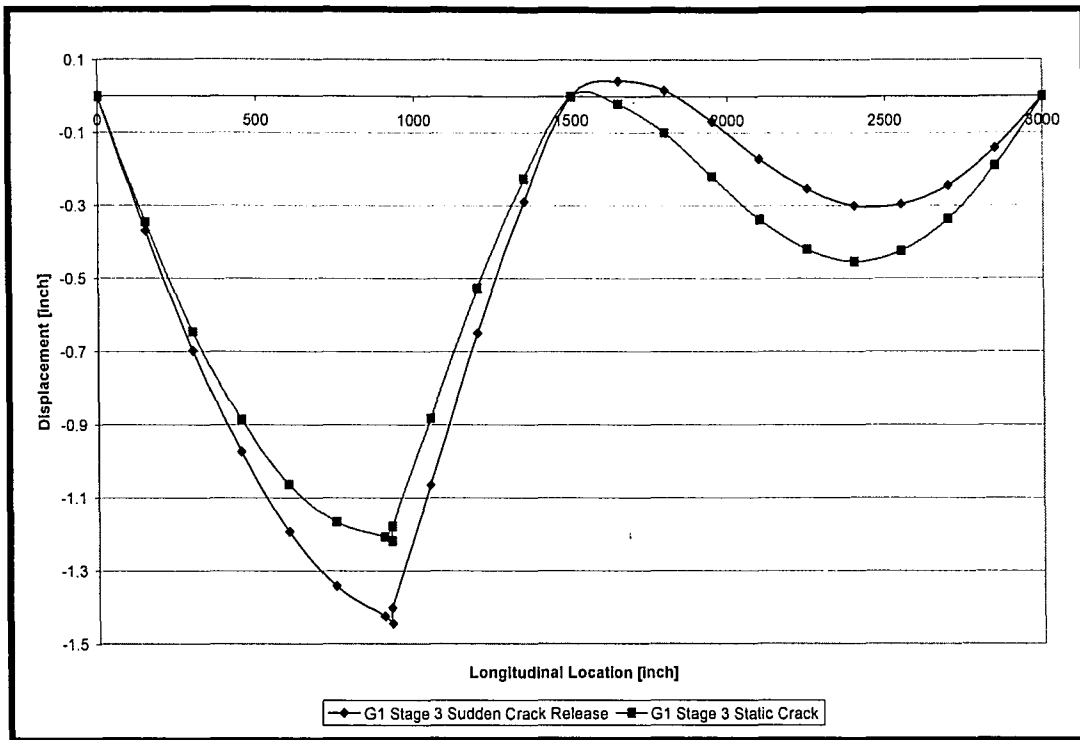


Figure 4.7: Stage 3 sudden crack release displacement versus Stage 3 static crack displacement

The stress distribution for the sudden crack release from Stage 1 to Stage 3 is roughly the same as the stress distribution for the static crack release despite the relatively large increase in deflection between the stages. Except the very localized yielding of the finite element modeling features at the pier, the connection of the lateral bracing members at the gusset plates, and the copes of the floorbeam ends, nowhere is a component of the steel superstructure subjected to any yielding. The maximum stress in G1 is about 20 ksi, in G2 is about 13 ksi, in the floorbeams is 7.55 ksi, in the stringers and diaphragms is 17.33 ksi, and in the lateral bracing is 9.18 ksi.

The concrete deck, as in the case of static release of Stage 3 cracking, has a region with a tensile stress higher than the specified tensile limit of 0.4 ksi. The size of this region for the sudden release of Stage 3 cracking is not any larger than the size of the region from the static Stage 3 crack (Figure 3.12). This status of the concrete deck does not induce failure or yielding of the steel components. The bridge is able to continue carrying the truck load.

4.3 Moving Truck Load

The moving truck is assumed to be moving at a speed of 61.36 mph (90 ft/s or 1080 in/s). The longitudinal movement of the truck's center axle is considered every 18 ft or 0.2 seconds. Shorter distance and time intervals, such as 9 ft and 0.01 seconds, would provide more precise results, but would require much longer times of computation. The first loading step is analyzed with the HS-20 center axle placed in line with the south abutment (this means that only the front and center axles are on the bridge span). The dynamic behavior of the two-girder bridge is examined at a time interval of 0.025 seconds for a time period of 0.2 seconds until the truck moves to its next location. The last loading step occurs when the HS-20 center axle is located at a longitudinal distance of 126 ft from the south abutment, just past the mid-span at 125 ft.

Analyzing the dynamic effect of a moving truck load for all stages of crack length offers a more realistic loading condition than the stationary truck load. It also provides a deflection response with higher deflection amplitude than that of static loading.

4.3.1 Stage 1 Dynamic Response to the Moving Truck Load

The displacement-time dynamic response to the moving truck load is only analyzed at the point of maximum deflection (at 56'-3" from the south abutment) as determined from Stage 1 static loading. This response is shown in Figure 4.8.

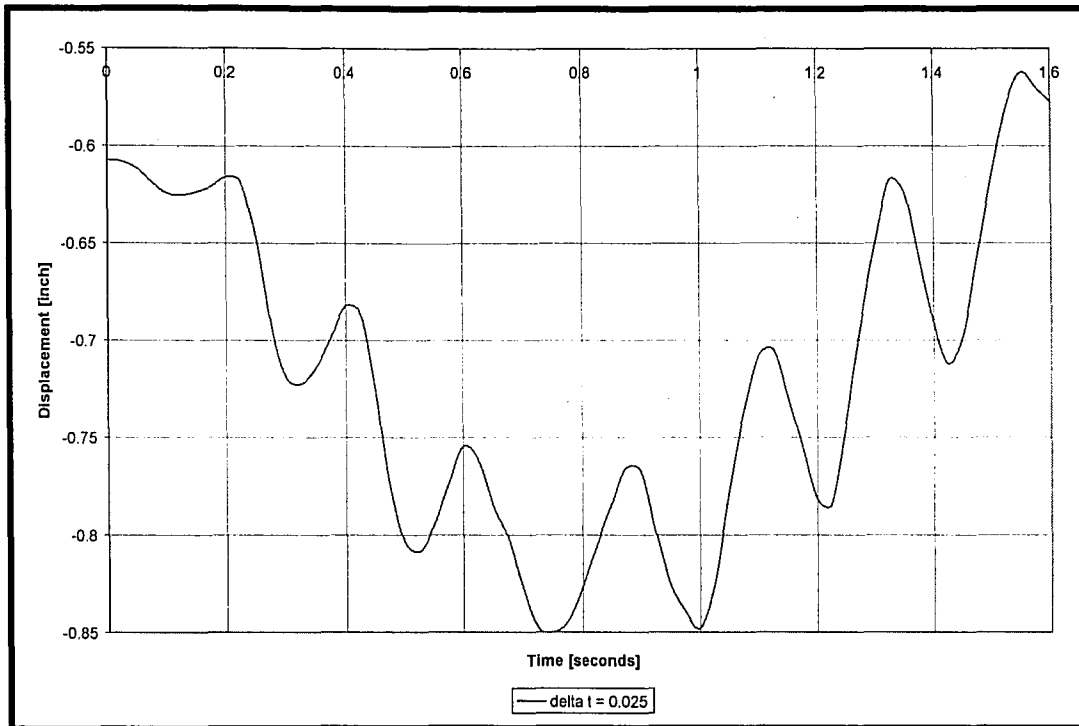


Figure 4.8: Stage 1 dynamic response of displacement at 56'-3" from the south abutment due to the moving truck load

As shown in Figure 4.8, the maximum dynamic displacement is 0.8499" occurring at 0.75 seconds. The truck has traveled to a point 2'-3" from the maximum displacement. Under static loading, the maximum displacement is 0.8009". The difference in displacement between the moving load dynamic response and the static load response is 0.049". That is an increase of 6%. Consequently, the displacement (and stresses) of the intact bridge (Stage 1) could be approximated from the Stage 1 static analysis.

4.3.2 Stage 2 Dynamic Response to the Moving Truck Load

The Stage 2 dynamic response to the moving truck load is again analyzed at the point of maximum deflection at 56'-3" from the south abutment as determined from Stage 2 static loading. The displacement-time response is shown in Figure 4.9.

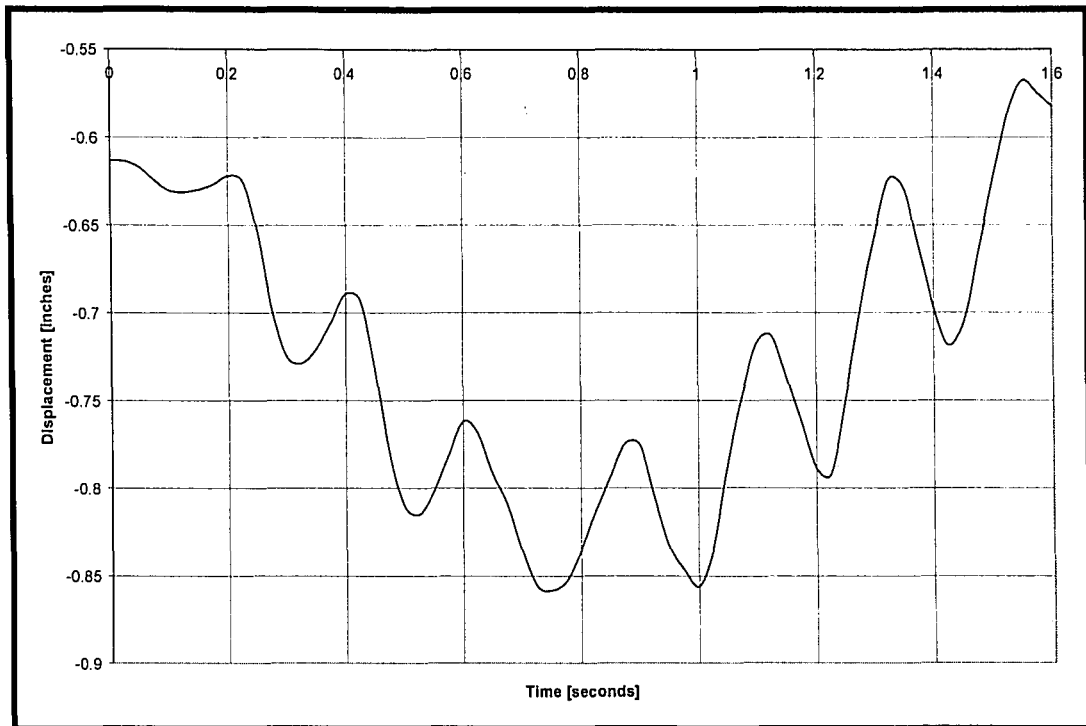


Figure 4.9: Stage 2 dynamic response of displacement at 56'-3" from the south abutment due to the moving truck load

As shown in Figure 4.9, the maximum dynamic displacement of 0.8583" occurs at 0.75 seconds for Stage 2 crack. The truck is at a location 2'-3" before the point of maximum displacement. These conditions are the same as for Stage 1. The maximum displacement at the same location under static loading for Stage 2 is 0.8095". The corresponding increase due to "impact" is 6%, being the same as for Stage 1.

In considering the dynamic response of the two-girder two-span continuous bridge with a flange crack (Stage 2) under moving load, it is expected that the

maximum deflection is higher than that when the flange is intact (Stage 1). The computed values are 0.8583" and 0.8499", respectively. That is an increase of 1%, being about the same percentage of increase between the two stages under static loading. Consequently, the displacement (and stresses) of the bridge with the flange cracked (Stage 2) could be approximated from the Stage 2 static analysis. Since the displacements are not excessive and the stresses in the bridge steel structure are all below the yield stress, the bridge could continue to function in-service with a crack in the girder flange.

4.3.3 Stage 3 Dynamic Response to the Moving Truck Load

The Stage 3 dynamic response to the moving truck load is analyzed at the point of maximum deflection (at the cracked cross section of the flange thickness transition) as determined from Stage 3 static loading. This response is shown in Figure 4.10.

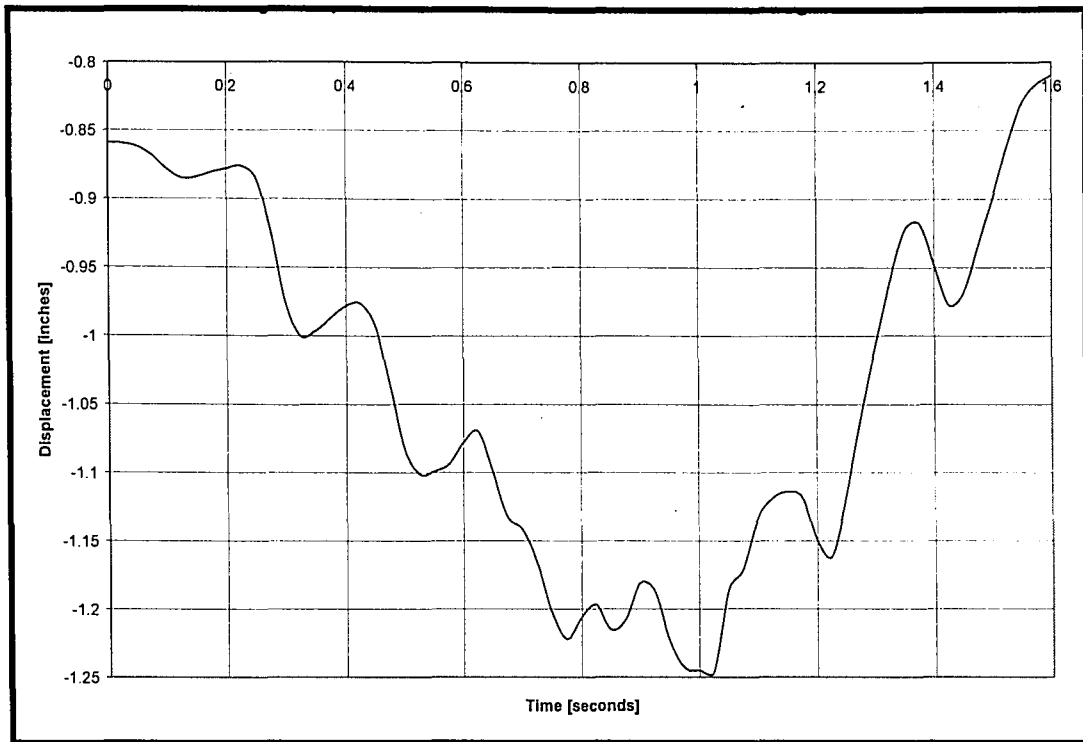


Figure 4.10: Stage 3 dynamic displacement response at the southern crack location to the moving truck load

As shown in Figure 4.10, the maximum dynamic displacement is 1.246” occurring at 1.025 seconds. The truck has traveled a distance of 90’, 13’ beyond the crack. The displacement at the same location under static loading for Stage 3 is 1.2186”. The increase is over 2%. This “impact” effect is smaller than that of Stage 2 and Stage 1 (at about 6%). To examine the effects of moving load further, the dynamic and static deflections of Stage 3 and Stage 1 are compared. The increase in dynamic and static deflections of Stage 3 and Stage 1 are compared. The increase in dynamic deflection from Stage 1 to Stage 3 is 46.6% (1.246” vs. 0.8499”). The increase in static deflection is 52.2% (1.2186” vs. 0.8009”). The static increase is higher. Again, the results suggest that the displacement (and stresses) of the bridge with a crack under truck load could be approximated from a static analysis.

Chapter 5: Bridge Response Comparison

5.1 Introduction

The objective of this preliminary study is to determine if the two-girder two-span continuous bridge will collapse if one girder fractures. The results ascertain that the bridge deflection is finite and the stresses in the steel superstructure are below yielding. The bridge does not collapse for any of the crack and loading situations analyzed. However, the situations analyzed are by no means comprehensive. Therefore, the displacements of various crack sizes and loading situations are compared to establish amplification factors. From these factors, the response of the bridge under the worse case scenario will be explored.

5.2 Amplification Factors

The amplification factors are based calculated using the displacements at the locations of their maximum value in the girder for each Stage of crack. Therefore, Stage 1 and Stage 2 amplification factors are based on the displacement values at a location 56'-3" from the south abutment of the cracked girder and Stage 3 amplification factors are based on the displacement values at the southern edge of the crack at 77'. Table 5.1 catalogs the maximum displacement values for all of the loading and crack sizes analyzed.

| | | Longitudinal Location | |
|----------------------|---------|-----------------------|------------------------------|
| | | 56'-3" | Southern Side of Crack (77') |
| Dead Load | Stage 1 | -0.6073 | - |
| | Stage2 | -0.6131 | - |
| | Stage 3 | - | -0.8592 |
| Dead and Live Load | Stage 1 | -0.8009 | - |
| | Stage2 | -0.8095 | - |
| | Stage 3 | - | -1.2186 |
| Sudden Crack Release | Stage 2 | -0.8155 | - |
| | Stage 3 | - | -1.4437 |
| Moving Truck Load | Stage 1 | -0.8499 | - |
| | Stage 2 | -0.8583 | - |
| | Stage 3 | - | -1.246 |

Table 5.1: Maximum girder displacement values

All of these loading and crack sizes have the dead load incorporated. The dead load deflections for the different stages of crack are the bases of comparison for all loading conditions of the respective crack stage. For instance, the amplification factor for the Stage 2 Static DL+LL condition is determined by dividing the displacement for that situation by the Stage 2 Static DL displacement. The result is an amplification factor for the effect of live load at Stage 2. This process is continued for all of the different loading conditions. The computed amplification factors are shown in Table 5.2.

| | | Longitudinal Location | |
|---------------------------------------|---------|-----------------------|------------------------------|
| | | 56'-3" | Southern Side of Crack (77') |
| Static LL Amplification | Stage 1 | 1.3187 | - |
| | Stage 2 | 1.3203 | - |
| | Stage 3 | - | 1.4182 |
| Sudden Crack Release LL Amplification | Stage 2 | 1.3301 | - |
| | Stage 3 | - | 1.6803 |
| Moving Truck LL Amplification | Stage 1 | 1.3994 | - |
| | Stage 2 | 1.3999 | - |
| | Stage 3 | - | 1.4502 |

Table 5.2: Amplification factors for the different analyzed loading conditions

The comparison of response by amplification factor can be made between stages of crack under the same loading condition and between loading conditions of the same stage of crack. From Stage 1 (with no crack) to Stage 2 (with the bottom flange cracked completely), the value of static live load amplification factor changes from 1.3187 to 1.3203, shown in Table 5.2. This increase is so trivial that the Stage 2 crack essentially has no effect on the displacement of the bridge. This same conclusion can be drawn from the moving truck live load. The value of amplification factor increases only from 1.3995 to 1.3999. From these very small differences in bridge response between the intact bridge (Stage 1) and the bridge with a flange crack (Stage 2), it can be concluded that the behavior of the two-girder two-span continuous bridge is little affected by a crack in a girder flange.

The increase in values of the amplification factor between Stage 2 and Stage 3 is much larger. The value changes from 1.3203 to 1.4182 for the stationary live load, from 1.3301 to 1.6803 for the sudden release of the crack, and from 1.3999 to 1.4502 for the moving truck. These large increases indicate the strong effects of the full depth crack on the bridge behavior.

A comparison of the amplification factor values among the different loading conditions reveals some interesting situations of the bridge being studied. The amplification factor values from Stage 1 and Stage 2 for all loading cases are all about the same (1.3187 to 1.3999). This consistency indicates that for this bridge the maximum displacements (and the corresponding stresses) are about the same whether induced by the sudden fracture of the flange or by the moving truck. On the other hand, for Stage 3 with a full depth crack of a girder, the static and moving truck loading cases have similar amplification factor values (1.4182 and 1.4502), while the value for the sudden fracture of the girder is higher (1.6803). This situation demonstrates that the behavioral effect on the bridge of the sudden fracture is more serious than the moving truck.

Regardless of these differences in behavior, the results from all cases indicate the bridge is not subjected to general yielding of any component (see Chapter 4). The bridge remains capable of carrying the truck under all loading conditions when there is a full depth crack in the girder.

5.3 Sudden Crack Release with Moving Truck Load

Although the response of the two-girder two-span continuous bridge is examined for fracture and moving truck, the combined effect is not. The

combination of a girder fracturing while a truck is traveling across the bridge creates a dynamic response of the bridge more severe than that of each load case. As indicated earlier, this preliminary study is not performing the analysis of the combined dynamic loads because of time constraints. However, an approximation of the bridge response is accomplished through the combination of the moving truck amplification factor and the sudden crack release amplification factor.

The static truck load for the sudden dynamic crack release is located with its centroid directly above the crack cross section location (77'). The dynamic moving truck load that creates maximum girder displacement is at the same location. Therefore, the amplification factors can be combined directly. The values of the two amplification factors for each stage of crack are multiplied to estimate an overall response. Table 5.3 shows the results of the combination.

| | | Longitudinal Location | |
|--|---------|-----------------------|------------------------------|
| | | 56'-3" | Southern Side of Crack (77') |
| Sudden Crack Release and Moving Truck Load Amplification | Stage 2 | 1.8621 | - |
| | Stage 3 | - | 2.4368 |

Table 5.3: Amplification factor for the sudden crack release and moving truck load

The maximum deflection of the girder under the combined influence of the crack release and the moving truck load for Stage 2 (flange crack) is calculated by multiplying the amplification factor (1.8621) by the dead load deflection (0.6161"). The result is a maximum girder deflection of 1.1417". For Stage 3 (full depth crack to the top of the girder web), the result is a maximum deflection of 2.0937". The

Stage 2 girder deflection under the combined influence of the crack release and the moving truck load is not noticeable. Although the Stage 3 girder deflection is over 2", the bridge remains capable of carrying truck loads.

In order to explore more the behavior of the bridge, the stress levels for Stage 3 need to be investigated. The region of a girder that is likely to experience yielding is around the mid-support. The stress contour for this region of the fractured girder is constructed by amplifying that of Stage 3 subjected to dead load. The multiplying factor is 2.4368, as listed in Table 5.2. Figure 5.1 is the resulting estimated stress contour.

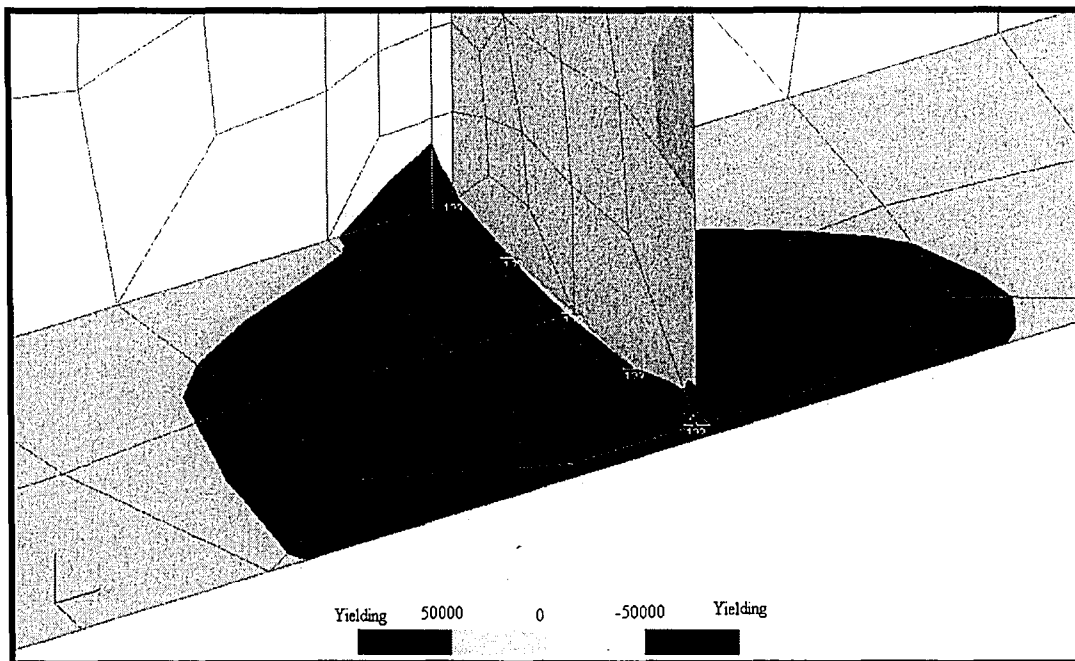


Figure 5.1: Estimated yielding region for Stage 3 combined crack release and moving truck load

Figure 5.1 shows that there is a small region of yielding. The yielding is still characterized as yielding in comparison to the size of the flange. The second region which is expected to sustain damage is the region of the concrete deck above the cracked girder (See Figure 3.12). However, the damage of the reinforced concrete

deck in a relatively small region is not expected to cause the bridge structure to collapse. Nowhere is a component of the steel superstructure subjected to any yielding. As determined by applying the Stage 3 amplification factor, the maximum stress in G1 is about 27.7 ksi, in G2 is about 22.0 ksi, in the floorbeams is about 8.21 ksi, in the stringers and diaphragms is about 17.9 ksi, and in the lateral bracing is about 12.4 ksi.

Based on the results of this amplification, the two-girder two-span continuous bridge is judged as redundant with respect to a sudden fracture of a girder.

Chapter 6: Conclusions and Recommendations

6.1 General Conclusions

The most important conclusion from the preliminary study on the redundancy of a two-girder two-span continuous bridge is that for all the cases examined, the bridge remains capable of carrying load. Under the most severe loading condition, there are areas that experience localized yielding of steel or failure of concrete. However, these regions are local. The two-girder two-span continuous bridge with a crack that extends to the top of the girder web remains stable and there is no catastrophic failure of the bridge.

As a result of these general conclusions, the classification of all two-girder bridges as “fracture-critical” is inaccurate. The AASHTO LRFD Bridge Design Specifications defines fracture critical as consisting of a fracture-critical member (FCM) or component in tension whose failure is expected to result in the collapse of the bridge or the inability of the bridge to perform its function (AASHTO, 2005). The analysis of this preliminary study demonstrates that the failure of the girder (FCM) will not result in the collapse of the two girder bridge. It is clear that specific provisions for after-fracture redundancy of girder bridges are a necessary addition to the AASHTO LRFD Bridge Design Specifications.

6.2 Stage 1 Conclusions

- The two-girder two-span continuous bridge is intact.

- Maximum deflection of a girder of the bridge under static dead and live load (HS-20 truck) is 0.8009" at a location 56'-3" from the south abutment. Under dead load alone, the deflection at this point is 0.6073".
- The maximum deflection in the girders for the moving HS-20 truck load is at the same location. This value is 0.8499".
- The stresses in the components of the steel superstructure and the concrete deck are all within the permissible limits.

6.3 Stage 2 Conclusions

- One girder of the bridge is assumed to have a cracked bottom flange at the transition thickness at 77' from the southern abutment.
- The maximum deflection of the cracked girder under static dead and live load is 0.8095" at the same location as Stage 1.
- The maximum deflection in the girders for the moving HS-20 truck load is at the same location. This value is 0.8583". The maximum deflection under the Stage 2 moving HS-20 truck is 1.3999 of that due to dead load alone.
- The maximum deflection in the girders for the dynamic release of the Stage 2 flange crack is located at the same point. This value is 0.8155". The amplification factor is 1.3301 as compared to the dead load deflection.
- Deflection due to sudden fracture of the flange is almost the same as that computed for the static release of the flange crack with the same loading.

This suggests that the deflection of the static crack release is a good estimate of that due to sudden fracture of a small crack.

- The combination effect of the moving HS-20 truck and dynamic crack release can be estimated by multiplying the amplification factors from each individual case. The result is an amplification factor of 1.8621 and a maximum deflection of 1.1417”.
- There is no general failure of material in any component of the steel superstructure, nor failure of the concrete.
- The two-girder two-span continuous bridge is able to carry the truck load without distress.

6.4 Stage 3 Conclusions

- The flange crack in one girder is assumed to extend to the top of the web. The girder is experiencing a full depth crack.
- Maximum deflection of the bridge under static dead load alone is located at the crack. This value is 0.8592”.
- Maximum deflection of the bridge under static dead and live load is also located at the crack. This value is 1.2186”.
- The maximum deflection in the girders for the moving HS-20 truck is located at the same point. This value is 1.246”. The Stage 3 moving HS-20 truck amplification factor is 1.4502 as compared to dead load alone.
- The maximum deflection in the girders for the dynamic release of the Stage 3 full depth crack is located at the crack. This value is 1.4437”.

The Stage 3 dynamic crack release amplification factor is 1.6803 as compared to dead load alone.

- The combination effect of the moving HS-20 truck and dynamic crack release can be estimated by multiplying the amplification factors from each individual case. The result is an amplification factor of 2.4368 and a maximum deflection of 2.0937" at the crack.
- The cracked girder is experiencing localized yielding at the mid-support. The bridge is also experiencing a region of tensile concrete failure near the crack location, when the bridge is subjected to the moving HS-20 truck and the dynamic crack release.
- Under the combined moving HS-20 truck and dynamic crack release, the bridge remains capable of carrying the truck.

6.5 Future Work

The analyses completed for this preliminary study are conducted using a two-girder two-span continuous bridge. Much more needs to be studied with regard to two-girder bridges being fracture critical. The following are some topics for future study:

- Dynamic analysis for the combined moving HS-20 truck and sudden crack release.
- Examine the deflection and stress of the bridge with a crack initiating from a gusset plate for lateral bracing and extending into the web.

- More in-depth examination of local stresses at member connections and bearings.
- Conduct non-linear analyses if needed, to capture the local and global behavior of the bridge after fracture occurs.
- Examine the after fracture behavior of a one-span two-girder bridge.
- Perform a parametric study to determine the influence of the location of the crack and the location and magnitude of load.
- Develop AASHTO specifications or commentary that gives guidelines for design and evaluation of redundancy in two-girder bridges.

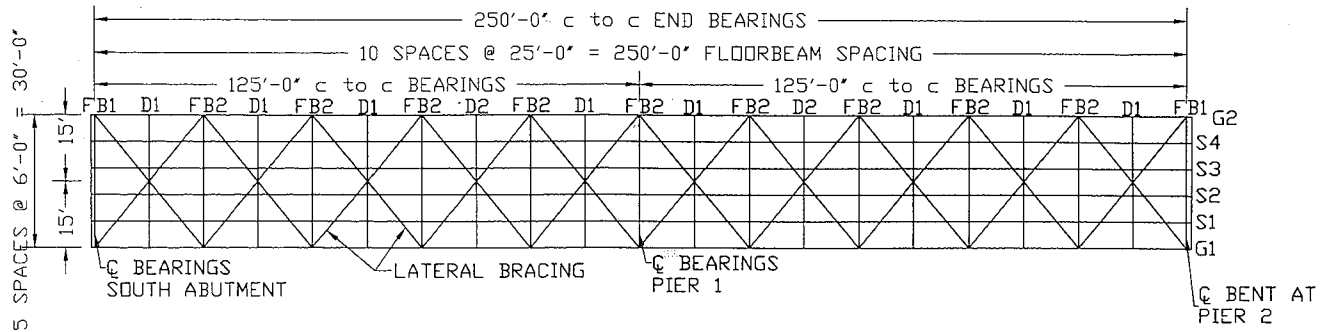
Appendix A: Two-Girder Two-Span Continuous Bridge Plans



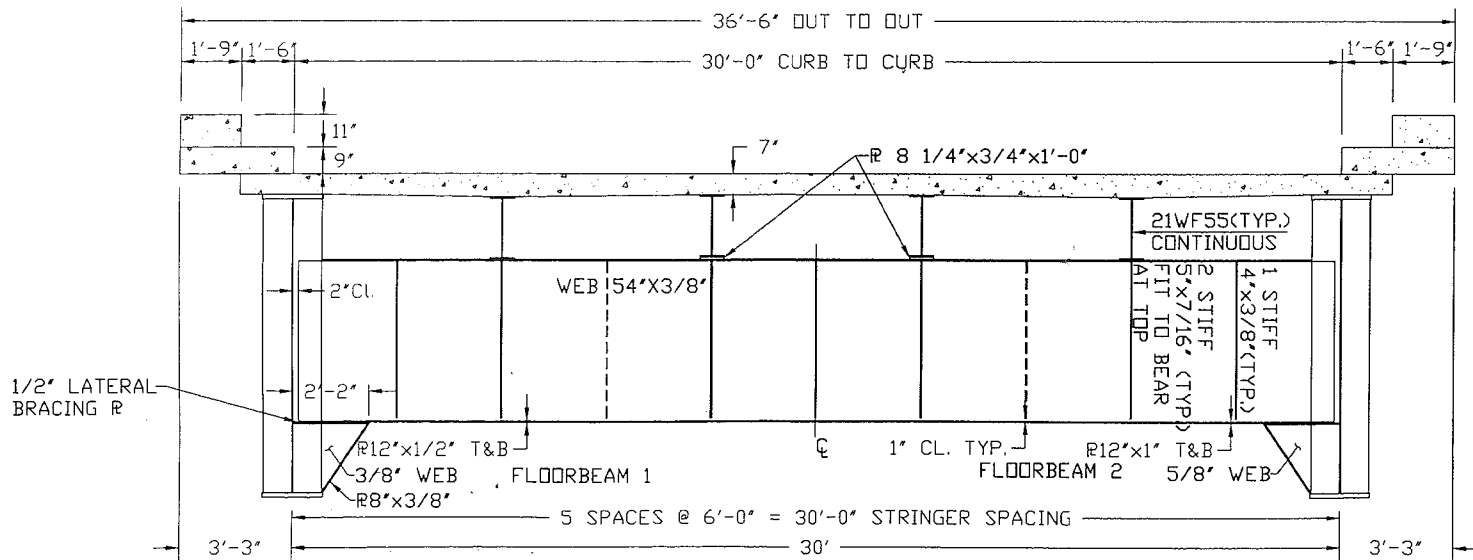
ADVANCED TECHNOLOGY FOR
LARGE STRUCTURAL SYSTEMS
117 ATLSS Drive
Lehigh University
Bethlehem, PA 18015
610-758-3535 FAX 610-758-6842

PROJECT:
**PILOT STUDY
ON
REDUNDANCY
OF A TWO-
GIRDER
TWO-SPAN
CONTINUOUS
BRIDGE UNDER
TRUCK LOADS**

SHEET NOTES:



STEEL FRAMING PLAN
SCALE: 1/32" = 1'-0"

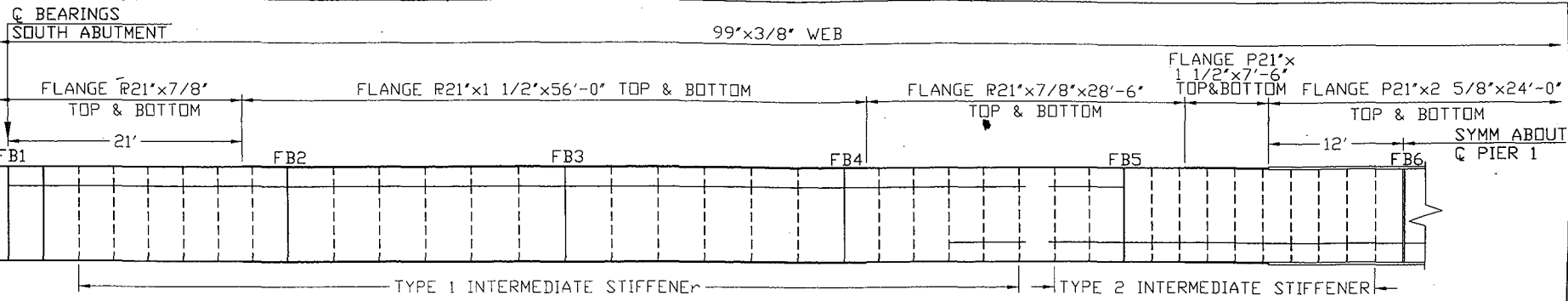


TYPICAL CROSS SECTION
SCALE: 1/4" = 1'-0"

DESIGNED BY:
DRAWN BY: SEM
CHECKED BY:
SCALE: AS SHOWN
DATE: 12/15/1961
PROJECT NO:
SHEET TITLE:

**FRAMING PLAN &
CROSS SECTION**

SHEET NO:



HALF GIRDER ELEVATION (EXTERIOR VIEW)
SCALE: 3/32"=1'-0"

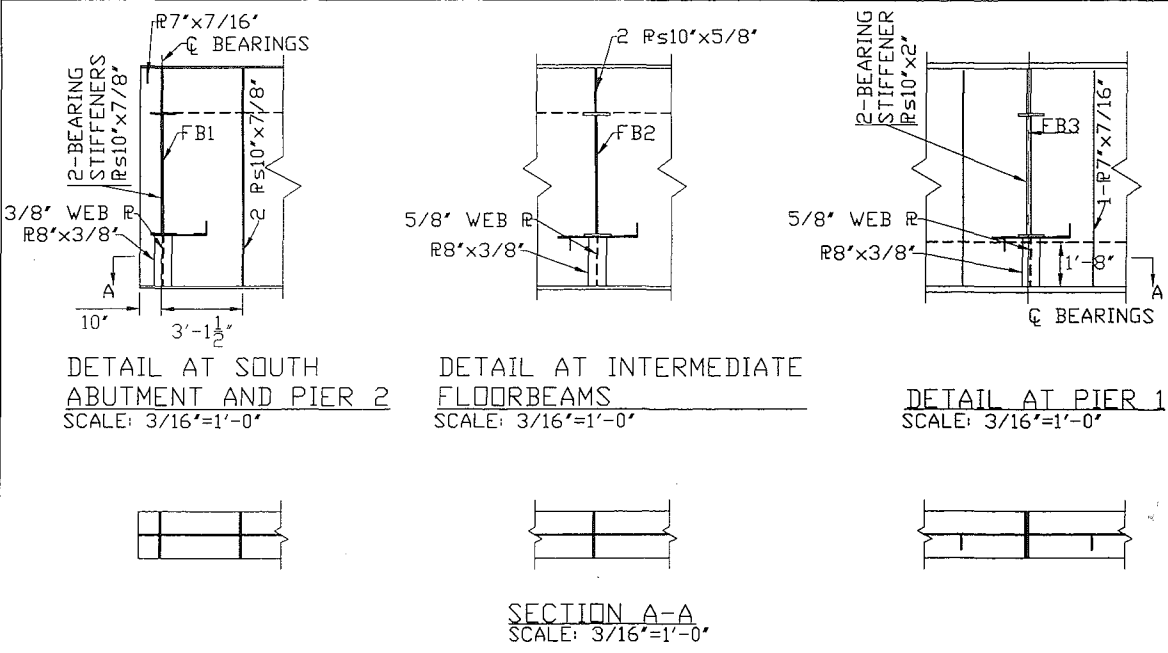
NOTE:
1. TYPE 1 STIFFENER R7"x7/16", WELD TO TOP FLANGE, 1" CLEARANCE AT BOTTOM FLANGE.
2. TYPE 2 STIFFENER R7"x7/16", WELD TO BOTTOM FLANGE, 1" CLEARANCE AT TOP FLANGE

ADVANCED TECHNOLOGY FOR
LARGE STRUCTURAL SYSTEMS
117 ATLSS Drive
Lehigh University
Bethlehem, PA 18015
610-758-3535 FAX 610-758-6842

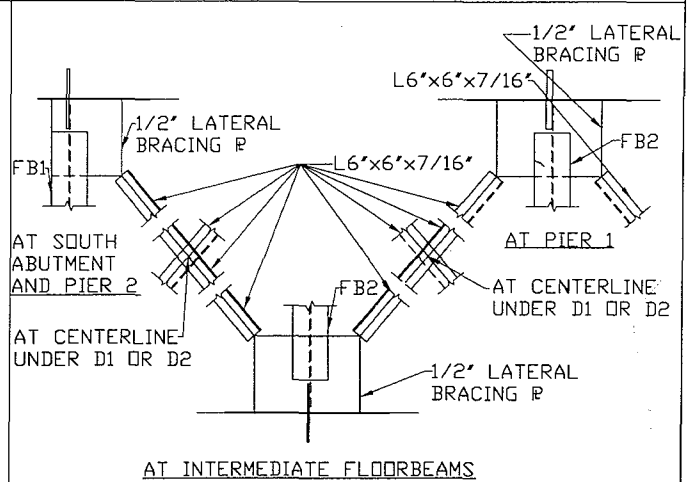
PROJECT:

PILOT STUDY
ON
REDUNDANCY
OF A
TWO-GIRDER
TWO-SPAN
CONTINUOUS
BRIDGE UNDER
TRUCK LOADS

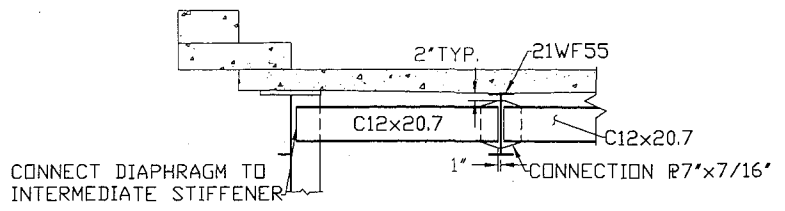
SHEET NOTES:



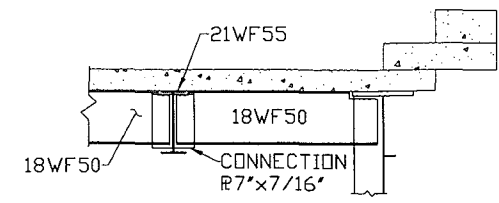
SECTION A-A
SCALE: 3/16"=1'-0"



LATERAL BRACING DETAILS
SCALE: 1/4"=1'-0"



PART SECTION SHOWING DIAPHRAGM 1
SCALE: 1/4"=1'-0"



PART SECTION SHOWING DIAPHRAGM 2
SCALE: 1/4"=1'-0"

| | |
|--------------|-------------|
| DESIGNED BY: | |
| DRAWN BY: | SEM |
| CHECKED BY: | |
| SCALE: | AS SHOWN |
| DATE: | 12/15/1961 |
| PROJECT NO.: | PROJECT NO. |
| SHEET TITLE: | |

GIRDER AND
MISCELLANEOUS
DETAILS

SHEET NO.:

References

1. ABAQUS/Standard User's Manual. Version 6.6, Hibbitt, Karlsson & Sorensen, Inc., Pawtucket, RI, 2006.
2. American Association of State Highway and Transportation Officials, AASHTO LRFD Bridge Design Specifications. Fourth Edition, AASHTO, Washington, D.C., 2007.
3. Chopra, Anil K., Dynamics of Structures. Second Edition, Prentice-Hall, Upper Saddle River, NJ, 2001.
4. Connor, Robert J., et al., "Inspection and Management of Bridges with Fracture-Critical Details". NCHRP Synthesis Report 354, 2005.
5. Cook, Robert D., et al., Concepts and Applications of Finite Element Analysis. Fourth Edition, John Wiley & Sons, Inc., Hoboken, NJ, 2002.
6. Daniels, J. Hartley, and Ressler, Stephen J., "After-Fracture Redundancy of Steel Bridges: A Review of Published Research". ATLSS Report No. 89-13, Lehigh University, Bethlehem, PA, 1989.
7. Fisher, John W., Fatigue and Fracture in Steel Bridges, Case Studies. John Wiley & Sons, Inc., Hoboken, NJ, 1984.
8. Ghosn, M., and Moses, F., "Redundancy in Highway Bridge Superstructures". NCHRP Project 12-36, March 1994.
9. Heins, C., and Hou, C.K., "Bridge Redundancy: Effect of Bracing". Journal of the Structural Division, Vol. 106, No. 6, June, 1980.
10. Heins, C.P., and Kato, H., "Load Redistribution of Cracked Girders". Journal of the Structural Division, Vol. 108, No. 8, August, 1982.
11. Hodgson, Ian C., et al., "Field Testing and Fatigue Evaluation of the Shippingport Bridge, Shippingport, PA". ATLSS Report, Lehigh University, Bethlehem, PA, 2006.
12. Lai, L.L.-Y., "Impulse Effect on Redundancy of a Tied-Arch Bridge". Computing in Civil Engineering, Proceedings of the First Congress held in conjunction with A/E/C Systems '94, Washington, D.C., June, 1994.

13. Structural Dynamics Research Corporation (SDRC), FEMAP User Guide.
January 2005.

7

Vita

Sarah Elizabeth Meagher was born on August 4, 1983 in New Rochelle, New York. She is the daughter of Kenneth Peter and Beth Anne Meagher and is the oldest of four girls. Her sisters are Caitlin, Brenna, and Eilis Meagher. Sarah graduated from Ridgefield High School in Ridgefield, Connecticut in 2001. She enrolled in Lehigh University in the fall of 2001 and obtained a Bachelor of Science in Civil Engineering in May, 2005 with high honors. Sarah continued her education at Lehigh University after receiving a Presidential Scholarship. She expects to graduate with a Master of Science in Structural Engineering in September, 2007. Sarah has accepted employment with Edwards & Kelcey and will work at their office in New York City.

Permanent Address:

261 Wilton Road West
Ridgefield, CT 06877
semb@lehigh.edu

END OF TITLE